1996

Development and evaluation of a graphite injector for inductively coupled plasma mass spectrometry

Preston Scott Clemons
Iowa State University

INFORMATION TO USERS

This manuscript has been reproduced from the microfilm master. UMI films the text directly from the original or copy submitted. Thus, some thesis and dissertation copies are in typewriter face, while others may be from any type of computer printer.

The quality of this reproduction is dependent upon the quality of the copy submitted. Broken or indistinct print, colored or poor quality illustrations and photographs, print bleedthrough, substandard margins, and improper alignment can adversely affect reproduction.

In the unlikely event that the author did not send UMI a complete manuscript and there are missing pages, these will be noted. Also, if unauthorized copyright material had to be removed, a note will indicate the deletion.

Oversize materials (e.g., maps, drawings, charts) are reproduced by sectioning the original, beginning at the upper left-hand corner and continuing from left to right in equal sections with small overlaps. Each original is also photographed in one exposure and is included in reduced form at the back of the book.

Photographs included in the original manuscript have been reproduced xerographically in this copy. Higher quality 6" x 9" black and white photographic prints are available for any photographs or illustrations appearing in this copy for an additional charge. Contact UMI directly to order.

UMI

A Bell & Howell Information Company
300 North Zeeb Road, Ann Arbor MI 48106-1346 USA
313/761-4700 800/521-0600

Development and evaluation of a graphite injector for inductively coupled plasma mass spectrometry

by

Preston Scott Clemons

A Dissertation Submitted to the
Graduate Faculty in Partial Fulfillment of the
Requirements for the Degree of
DOCTOR OF PHILOSOPHY

Department: Chemistry
Major: Analytical Chemistry

Approved:

Signature was redacted for privacy.

In Charge of Major Work

Signature was redacted for privacy.

For the Major Department

Signature was redacted for privacy.

For the Graduate College

Iowa State University
Ames, Iowa

1996

TABLE OF CONTENTS

CHAPTER 1. GENERAL INTRODUCTION

The phases an analytical method goes through have been compared to the seven ages of man.[1] Inspiration for this comparison comes from the play written by William Shakespeare in 1598, *As You Like It*.[2] These ages by Laitinen and Shakespeare are listed in Table 1. Inductively coupled plasma mass spectrometry (ICP-MS) has been assigned these ages in a recent paper.[3] As with man, the actual conception of ICPMS is uncertain but some events can be traced to its origin. Mass spectrometry was applied to flames[4] and d.c. plasmas[5] in the mid-70's. This is about ten years after the ICP was introduced as an analytical tool.[6,7] All doubt of the occurrence of conception was erased in 1980 when Houk et. al. gave birth to the first research instrument.[8] Commercial instruments followed around 1983 from Sciex and VG Elemental. From the mid-80's to the early 90's papers characterizing the technique flooded journals, many of which can be found conveniently referenced in books about the subject.[9,10]

It is believed that ICP-MS has matured and reflection for future directions is the current course of this technique.[3] Recent innovations in the mass spectrometer end of ICP-MS confirm this.[11-13] Recent work on fundamental properties like ion production and transport suggest the phase of instrument characterization has not fully passed.[14] Old problems like

Table 1. A. Seven ages of man by Shakespeare in the play, *As You Like It*. B. Seven ages of an analytical method by Laitinen. Reproduced with permission from reference 3.

A. The seven ages of man - Shakespeare

1st	the Infant
2nd	the School Boy
3rd	the Lover
4th	the Soldier
5th	the Justice
6th	the Retired Gentleman
7th	the Old Man

B. The seven ages of analytical method - Laitinen

1st	Conception of the idea
2nd	First research instruments
3rd	First commercial instruments
4th	Characterization of method
5th	Maturity
6th	Reflection
7th	Old age and senescence

polyatomic ion interferences continue to be revisited.[15] In summary, the technique is moving toward new horizons while people strive to better understand the problems and fundamental operation of the overall device. With this type of interest, ICP-MS will not reach the last phase, senescence, for some time.

This general introduction will continue by discussing some virtues of the ICP that make it a good source for elemental mass spectral analysis. Problems remain that leave room for fundamental and applied research and keep ICP-MS away from senescence. The problem area of mass overlap of analyte ions and metal oxide ions will be dealt with. The approaches taken to eliminate or at least reduce these interferences will be discussed.

The ICP: A Source of Ions

The ICP is a hot, partially ionized gas, usually argon, sustained inside a quartz torch. Figure 1 illustrates a typical torch and the corresponding gas flows. This torch is nestled inside a few turns of copper tubing, called the load coil, which is typically cooled by flowing water of high electrical resistance. The load coil is supplied with radio-frequency (RF) current from a generator typically operated at either 27 or 40 MHz.

Added electrons from a Tesla coil interact with the time

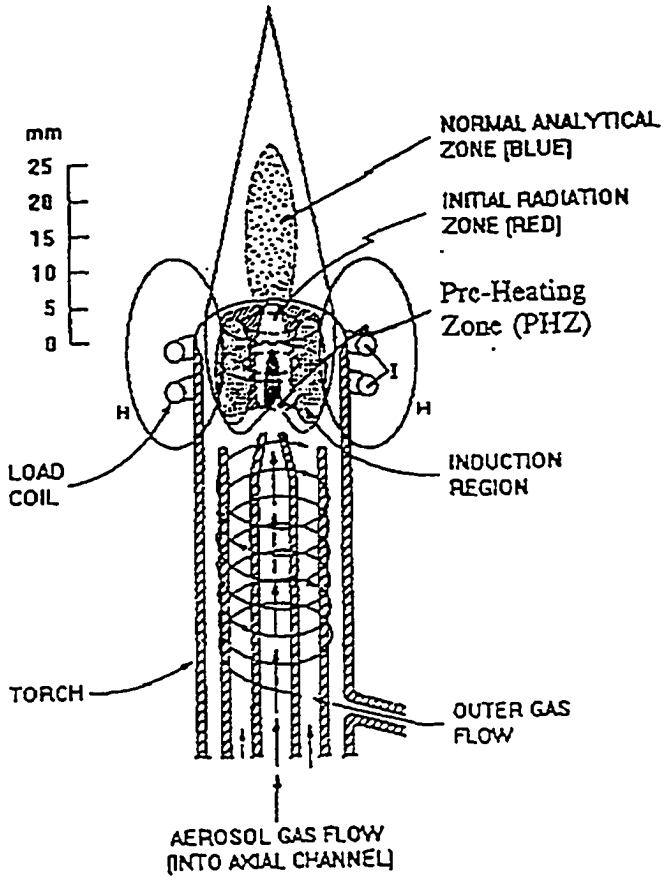

Figure 1. Typical ICP torch showing argon gas flows used and emission zones produced by yttrium. The initial ratidiation zone (IRZ) is produced by neutral yttrium oxide and atoms (red). The NAZ is produced by yttrium ions (blue). Reproduced with permission from reference 46.

varying magnetic field about the load coil within the torch. In this way, electrical energy of the load coil is transformed into kinetic energy of the added electrons. This process of harnessing the energy of the load coil is called inductive coupling. The area of the plasma where this occurs is the induction region. In addition to inductive coupling, at any time there is a potential difference that exists along the length of the turns of the load coil. Electrons and ions accelerated through this potential difference experience capacitive coupling, a minor path of energy introduction.

At atmospheric pressure the electrons have a short mean free path of about $5x10^{-8}$ m. As a result, these energetic electrons experience frequent collisions to produce excited neutral argon atoms and argon ions. These species will continue to collide and produce more excited neutrals, ions and electrons, which heats the gas and sustains the plasma.

There are generally three routes that a neutral ground state analyte atom, M^0, can take to become an ion, M^+. These are summarized in the following equations:

1. Electron Impact (1)

$$M^0 + e^-_{fast} \rightleftharpoons M^+ + 2e^-_{slow}$$

2. Penning Ionization (2)

$$Ar^* + M^0 \rightleftharpoons M^+ + Ar + e^-$$

3. Charge transfer (3)

$$Ar^+ + M^0 \rightleftharpoons (M^+)^* + Ar$$

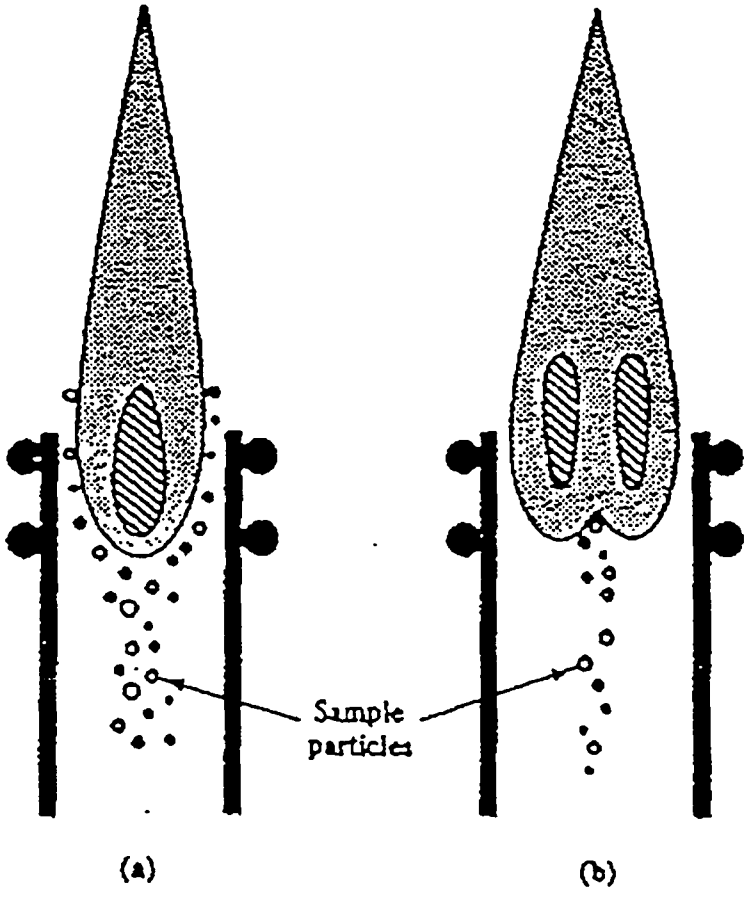

Figure 2. a) A 5 MHz ICP showing the centralized tear drop induction region. b) A 27 MHz ICP with the "doughnut" or toroidal shaped induction region. Reproduced with permission from reference 45.

Electron impact occurs when M^0 collides with fast electrons created from the induction field about the load coil. Penning ionization is a result of an argon-metastable atom, Ar*, colliding with and transferring its excited state energy to a ground state analyte atom, M^0. Argon has relatively high excitation energies, 11.55 and 11.76 eV. This reaction is favorable for a number of elements which have ionization energies that are lower than the above mentioned excitation energies for argon.

The charge transfer reaction occurs when the excited state analyte ion has an energy level that closely matches the ionization energy of argon. Reaction 3 is not a dominant ionization mechanism but can supplement the ion population produced by reactions 1 and 2. When the analyte ion, $(M^+)^*$, relaxes to its ground electronic state the result is a release of energy by emission of a photon. Thus, the above ionization mechanisms are also excitation mechanisms that are useful for atomic emission spectrometry (ICP-AES).

The ICP is a good source of ions for elemental analysis. The percent ionization for elements of the periodic table have been calculated using accepted values of electron density and ionization temperature.[16] Most metals are about 90-100% ionized which favors their determination by ICP-MS.

Structure of the ICP

The early days of ICP development used lower frequency current that failed to produce a distinct annular region low in the plasma. Figure 2 compares an ICP operated at 5 MHz and 27 MHz respectively. The lower frequency plasma does not allow the sample to pass through the "hot" region. With this ICP the sample aerosol dribbles around the cooler outside region. At higher frequencies an annulus or toroid forms in the induction region that allows the aerosol gas to pass through the center of the induction region and carries the sample aerosol through the "central channel".

This development is significant in several ways. It allows the sample to pass through the part of the plasma where desolvation, vaporization, atomization, excitation and ionization are most efficient. This centralized aerosol stream does not greatly affect the outer portion of the plasma where the induction process occurs. Thus, the sample matrix components can change greatly without a major change in the bulk plasma. Finally, Figure 1 shows that the analyte is confined for convenient collection of photons for AES analysis or ions for MS analysis.

Figure 1 also shows several distinct regions of the central channel. These zones are best described when observing emission from a concentrated solution of yttrium. As the sample aerosol leaves the injector it enters a hot

region at the base of the plasma. Desolvation begins here and this region is often called the pre-heating zone (PHZ). Next, a bullet shaped area (which is actually pink to red in color) can be seen. This is a result of emission from yttrium atoms and undissociated yttrium oxide molecules. This region of emission is often referred to as the initial radiation zone (IRZ). This area of the plasma is not a desirable place to sample for mass spectral analysis as it is low in analyte ion density and has lots of MO^+. The final analyte region is the normal analytical zone (NAZ). The blue color (not apparent from Fig. 1) is a result of emission from yttrium ions. Most optical measurements are made here and given that the ion density is high, sampling for mass spectral analysis is also done here. Notice that the NAZ rapidly expands after the IRZ to fill the entire central channel. Because of this the sampling orifice must be placed very close to the tip of the IRZ, not in it, to collect as many ions as possible. Unfortunately, this can lead to sampling oxide ions of the analyte and this could lead to spectral interferences.

General Interferences

In 1933, G. E. F. Lundell wrote an article called "The Chemical Analysis of Things as They Are."[17] Lundell commented:

> There is no dearth of methods that are entirely satisfactory for the determination of elements when

they occur alone. The rub comes in because elements never occur alone, for nature and man frown on celibacy. Lundell must have been a prophet for this is very true for ICP-MS. The matrix of the sample, argon and solvent atoms can all lead to certain types of interferences, which diminish the elemental selectivity of the device.

There are generally two types of interferences associated with ICP-MS, spectral and non-spectral. Non-spectral interferences result from matrix effects caused by space charge or clogging of the sampling cone. Spectral interferences are more pertinent to this dissertation. The majority of ICP-MS devices available today use a quadrupole as the mass analyzer. This device operates at or about unit mass resolution. Because of this, the mass to charge ratio corresponding to an analyte ion can be obscured by any specie of the same nominal mass to charge ratio.

Two elements with isotopes of the same nominal mass would cause a spectral interference. Determination of calcium in an argon ICP is difficult because of such an interference. Both elements share their major isotopes at mass 40, ^{40}Ca (97.0%) and ^{40}Ar (99.6%). Another type of spectral interference is from doubly charged matrix ions. The quadrupole filters ions by their mass to charge ratio (m/z). An element like ^{138}Ba that has lost two electrons would appear in the mass spectrum at m/z = 69. Unfortunately gallium's major isotope, ^{69}Ga

(60.9%), is also at this m/z value.

Furthermore, although the plasma is an efficient atomization cell some polyatomic ions persist and cause interferences. Species of argon are a major contributor to this group of spectral interferences. Mineral acids can cause formation of ArX^+ ions such as $^{40}Ar^{35}Cl^+$, which interferes with the only isotope of arsenic, $^{75}As^+$. Argon can form a dimer to produce $^{40}Ar_2^+$ which interferes with $^{80}Se^+$. Fortunately, alternative isotopes exist for selenium, yet at lower relative abundance. Iron at m/z= 56 has a problem with $^{40}Ar^{16}O^+$. Iron has another isotope at m/z= 54 but $^{40}Ar^{14}N^+$ can be a problem if nitric acid is part of the acid matrix.

Aside from polyatomic ions with argon, others exist. Sulfur, generally from sulfuric acid, can form SO^+, SO_2^+ and SO_3^+, which in turn interferes with the determination of Ca, Zn, and Se.

The previously mentioned spectral interferences in ICP-MS are only representative of the general problem. Lists of polyatomic ions and interfered elements are available.[18,19] A final group of polyatomic ions, metal oxides (MO^+), will be discussed for its importance to this dissertation. The following scenario should help to illustrate why MO^+ are baneful to many elemental determinations. The analysis of geological materials for rare earth elements (REE) has been a common task for ICP-MS[20-22]. Geologists are often interested in

trace levels of heavy REE (HREE) in a large concomitant matrix of light REE (LREE). Most samples contain much higher levels of LREEs than HREEs. Unfortunately, some monoisotopic REE's exist, most of which are HREE. If a HREE like holmium, ^{165}Ho (100%), is to be determined in a matrix of concentrated samarium, $^{149}Sm^{16}O^{+}$ causes an interference problem . This isotope of samarium, ^{149}Sm, is fairly abundant (13.8%), so the resulting metal oxide ion would be detrimental to the determination of holmium.

Metal Oxides: Search and Destroy

There is a debate over where MO^{+} ions actually originate. Some believe that analyte oxides remain in the plasma and are not fully dissociated[23]. Others think that they are a result of boundary layer reactions[24,25]. Further, there are those that blame the interface region between the sampler and skimmer.[26-27]

The last point may or may not seem reasonable. It is estimated that an atom or ion collides with argon atoms about 250 times in the free jet expansion behind the sampling cone.[28] If oxygen is present at $1x10^{16}$ cm^{-3} then an M^{+} ion collides with an oxygen atom about twice in this region. Thus, there is probably little or no MO^{+} produced in an ideal supersonic jet. However, Niu et al. have proposed that a shock wave might exist in front of the skimmer orifice.[29] There could be enough collisions here to produce some MO^{+}.

The boundary layer is a cool layer of gas which forms across the sampling cone face. In this layer a sheath of positive ions collects at the surface of the cone due to the higher mobility of electrons. This cool gas layer has an excess of positive ions and is a good region for analyte ions to react with oxygen atoms and form MO^+.[24,25] Attention has been directed toward the interface design to reduce the ratio of MO^+ to M^+ ions. The skimmer orifice is generally kept smaller than the sampling orifice to reject the extra MO^+ made in the boundary layer.[30] Others have shown that the condition of the orifice is important; polishing the inside of the sampling cone attenuated a number of polyatomic ions.[31]

The ICP is thought of as an efficient atomization cell. It is possible that some analyte oxides do not dissociate before being sampled by the interface. Recall, the IRZ is a region of analyte atom and analyte oxide emission. Also remember, for optimum sampling of analyte ions the sampling cone must be as close to the IRZ as possible because the NAZ quickly becomes diffuse in the central channel. This is unfortunate as some analyte oxide ions may be sampled before entering the "hottest" part of the central channel to be dissociated. This is also true if the sample introduction system allows large wet droplets to pass into the plasma. Analyte oxides probably exist in the vicinity of these droplets as they pass through the plasma. The presence of the

droplet cools its immediate neighborhood, so the oxides remain.

Plasma operating conditions are known to affect the level of MO^+ in an ICP-MS spectrum. Forward power, aerosol gas flow rate, and sampling position have all been investigated.[32] It would be ideal to set these parameters to achieve maximum ion signal. The general problem with this approach is illustrated in Figure 3. The MO^+ signal is still 50% of its maximum under operating conditions that yield maximum analyte ion signal.

The size and position of the IRZ are dependent on the forward power and aerosol gas flow rate. Visual inspection of the IRZ while nebulizing concentrated yttrium and adjusting these parameters shows this. If the position of the IRZ changes the optimum sampling position will change and so will the level of MO^+ sampled by the interface. It is possible to optimize plasma operating and sampling conditions and add certain gases to the plasma to reduce MO^+. Addition of certain molecular or noble gases to the central channel reduces many polyatomic ions.[33,34] Also, addition of N_2 gas to the plasma gas has shown some success.[35] It is possible that some of the added gases help to more efficiently couple energy to the center of the plasma to aid in the dissociation of these dreaded analyte oxides.[36]

Conventional sample introduction requires making an aerosol from an aqueous analyte solution. This solvent

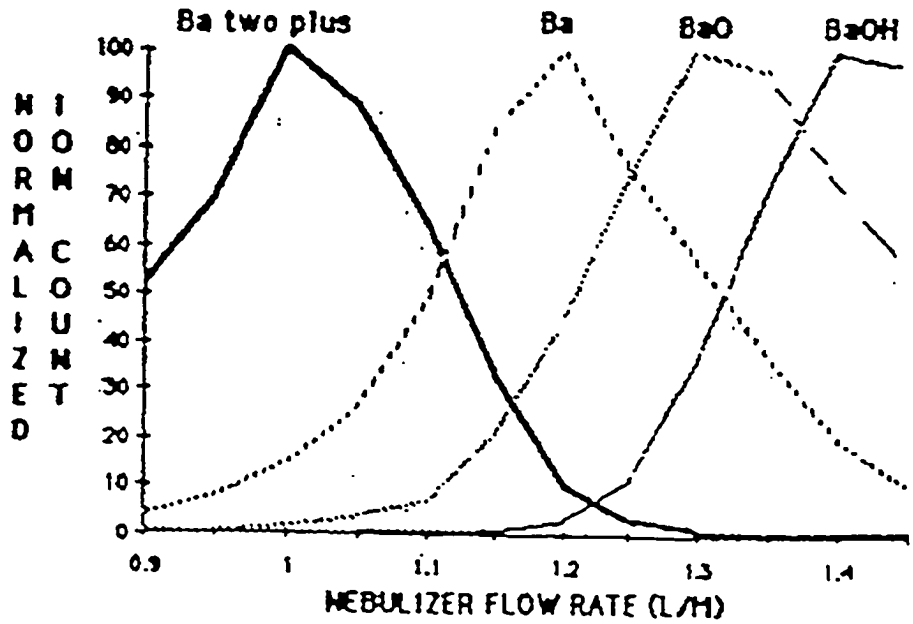

Figure 3. Plots of signal for Ba+2, Ba+, BaO+ and BaOH+ as a function of aerosol gas flow rate (AGFR). Notice, the signal for BaO+ is about 50% of its maximum at an AGFR yielding maximum Ba+ signal. Reproduced with permission from reference 31.

provides a source of oxygen atoms. It has been proven that removal of this source of oxygen can dramatically reduce the level of MO^+ observed in the mass spectrum. This effort centers around employing sample introduction methods that prevent aqueous solvent from entering the plasma. A cooled spray chamber condenses some water vapor,[37] yet cryogenic desolvation has proven to be more aggressive and fruitful in reducing the MO^+ problem.[38] Membrane desolvation has been employed with similar success.[39] Laser ablation[40] (LA), and direct sample insertion[41] (DSI) are methods that introduce a solid sample. Electrothermal vaporization (ETV) has the advantage of separating the solvent from the analyte in the vaporization cell.[42] Sample introduction systems that produce a transient signal often produce results with sub-standard precision for most mass spectrometers.[43]

Specialized sample introduction devices are good for instrument companies but not really practical for the average laboratory. The privileged few can afford a high resolution ICP-MS device that utilizes a magnetic sector for mass analysis. This level of selectivity almost eliminates the problem of spectral interferences caused by polyatomic ions. From the earlier discussion in this general introduction, the ICP is a good source of ions for mass spectral analysis. The interference caused by polyatomic ions is a major problem for a quadrupole ICP-MS device. There is a need for a simple,

cheap, easy-to-maintain method that provides relief from the interferences created by analyte oxide ions.

Dissertation Objectives and Organization

This dissertation is presented such that each chapter stands alone as a complete scientific manuscript with accompanying references, tables and figures. Each chapter is a paper either published in or submitted to a research journal.

Chapter 2 introduces an injector device for a demountable torch that utilizes a graphite tube supported by a stainless steel tube. This graphite tube is inserted into the base of the operating plasma. The most surprising result from this device is that the operating conditions for optimum analyte ion signal also minimize the analyte oxide ion signal. This device requires a much lower aerosol gas flow rate than the normal quartz injector. Rinse out curves show that this does not greatly affect memory in the nebulization and desolvation system. Another beneficial result is that there is general enhancement for all analyte signals. Some analyte signals show greater enhancements than others, especially certain important elements with high ionization energies.

Chapter 3 attempts to characterize the polyatomic ion background produced by the device, aside from analyte oxide ions. Many times a remedy for a specific interference either

creates new problems or makes existing ones worse. The spectrum from m/z= 10 to 81 was investigated. The basic features of the lower mass range, m/z= 10 to 38, only receive comments explaining what species are present. The appearance of a significant peak at m/z= 28 suggests that $^{12}C^{16}O^+$ is formed from the carbon evolved from the graphite injector. Also, the $^{16}O_2^+$ signal is greatly attenuated relative to that produced by a normal quartz injector. The mass region from m/z= 45 to 81 typically contains noxious polyatomic ion interferences that are described using the concept of background equivalent concentration (BEC). The interference from $^{40}Ar^{12}C^+$ is much worse using the graphite injector compared to the normal quartz injector. Measurements of $^{52}Cr^+$ are almost impossible because of this polyatomic ion. Fortunately, chromium has other isotopes available. A benefit to using the graphite injector is that the chlorine containing polyatomic ions are attenuated. The BEC values for $^{35}Cl^{16}O^+$ and $^{40}Ar^{35}Cl^+$ improve by a factor of 7 and 17 respectively. The final quest of this chapter is to assess the severity of matrix effects. It seems the problem is no worse with this device than is expected from the typical quartz injector. A remedy for correcting this problem is borrowed from a predecessor and used with success[44].

The purpose of chapter 4 is to connect some relevant theory about graphite furnace atomization to how this device produces its low level of MO^+. In the graphite furnace, many

analytes are atomized, in part, through reduction of their oxide by carbon. This process is favorable in the higher temperatures of the furnace. Our estimates suggest the graphite injector tip operates at about the same temperature as a graphite furnace. Our data show there is a direct correlation between the carbon density in the plasma and the level of metal oxide ions observed. Finally, there is evidence that a charge transfer reaction could be responsible for ion signal enhancements seen for certain elements. These enhancements can be directly linked to the density of carbon in the plasma.

References

1. Latinen, H. A. *Anal. Chem.* 1973, 45, 2305.
2. Rause, A. L. *The Annotated Shakespeare*, Greenwich House, New York, 1988, 360.
3. Horlick, G. *J. Anal. At. Spectrom.*, Part B, 1994, 4, 593.
4. Hayhurst, A. N.; Telford, N. R. *Combust. Flam.* 1977, 28, 67.
5. Gray, A. L. *Analyst* 1975, 100, 289.
6. Wendt, R. H.; Fassel, V. A. *Anal. Chem.* 1965, 37, 920.
7. Greenfield, S.; Jones, I. L. I. *Analyst*, 1964, 89,713.
8. Houk, R. S.; Fassel, V. A.; Flesch, G. D.; Svec, H. J.; Gray, A. L.; Taylor, C. E. *Anal. Chem.* 1980, 52, 2283.

9. Taylor, H. E.; Carbarino, J. R. in *Inductively Coupled Plasmas in Analytical Atomic Spectrometry*, 2nd Ed., eds. Montaser A.; Golightly, E. W., VCH, New York, 1992, pg. 651.

10. Jarvis, K. E.; Gray, A. L.; Houk, R. S. *Handbook of Inductively Coupled Plasma Mass Spectrometry*, Chapman and Hall, New York, 1992.

11. Warren, A.; Allen, L. A.; Pang, H.M.; Houk, R. S.; Jangorbani, M. *Appl. Spectrosc.* 1994, 48, 1360.

12. Hieftje, G.; Mahoney, P. paper presented at the 22nd annual conference of the Federation of Analytical Chemistry and Spectroscopy Societies, Cincinnati, OH., 15-20 October, 1995.

13. Koppenal, D. W.; Barinaga, C. J.; Smith, M. R. *J. Anal. At. Spectrom.* 1994, 9, 1053.

14. Nonose, N.; Masaaki,K paper presented at the 22nd annual conference of the Federation of Analytical Chemistry and Spectroscopy Societies, Cincinnati, OH., 15-20 October, 1995,.

15. Olesik, J. W.; Dziewatkoski, M; McGowan, G.; Thaxton, K. paper presented at the 22nd annual conference of the Federation of Analytical Chemistry and Spectroscopy Societies, Cincinnati, OH., 15-20 October, 1995, No. 222.

16. Houk, R. S. *Anal. Chem.* 1986, 58, 97A-105A.

17. Lundell, G. E. F. *Ind. Eng. Chem*, Anal. Ed. 1933,5, 221.

18. Vaughan, M.; Horlick, G. *Appl. Spec.* 1986, 40, 434.

19. Alves, L. C. Cryogenic Desolvation for Sample Introduction into Inductively Coupled Plasma Mass Spectrometry, Ph.D. thesis, Iowa State University, Ames, IA., 1993, Appendix I.

20. Longerich, H. P.; Fryer, B. J.; Strong, P. F.; Kantipuly, C. J. *Spectrochim. Acta*, Part B, 1987, 42B, 75.

21. Lichte, F. E.; Meir, A. L.; Crock, J. G. *Anal. Chem.* 1987, 59, 1150.

22. Jarvis, K. E. *Chem. Geol.* 1988, 68, 31.

23. Hobbs, S. E.; Olesik, J. W. *Spectrochim. Acta*, Part B, 1993, 48, 817.

24. Olivares, J. A.; Houk, R. S. *Anal. Chem.* 1985, 57, 2674.

25. Gray, A. L. *Spectrochim. Acta*, Part B, 1986, 41B, 151.

26. Gray, A. L.; Williams, J. G. *J. Anal At. Spectrom.* 1987, 2, 81.

27. Wilson, D. A.; Vickers, G. H.; Heiftje, G. M. *J. Anal. At. Spectrom.* 1987, 2, 227.

28. Douglas, D. J.; French, J. B. *Spectrochim. Acta*, Part B, 1986, 41B, 197.

29. Niu, H. S.; Houk, R. S. *Spectrochim. Acta*, Part B, 1990, 45B, 453.

30. Vaughan, M. A.; Horlick, G. *Appl. Spectrosc.* 1986, 40, 434-445.

31 Hutton, R. U.S. Patent No. 4760253, 1988.

32. Vaughan, M. A.; Horlick, G. *Appl. Spectrosc.* 1986, 40, 434.

33. Evans, E. H.; Ebdon, L. J. *J. Anal. At. Spectrom.* 1990, 5, 425.

34. Smith, F. G.; Wiederin, D. R.; Houk, R. S. *Anal. Chem.* 1991, 63, 1458.

35. Lam, J. W.; McLaren, J. W. *J. Anal. At. Spectrom.* 1988, 3, 743.

36. Murrillo, M.; Mermet, J. M. *Spectrochim. Acta*, Part B, 1989, 44B, 359.

37. Crain, J. S.; Gillmore, D. L. *Appl. Spectrosc.* 1992, 46, 547.

38. Alves, L. C.; Wiederin, D. R.; Houk, R. S. *Anal. Chem.* 1992, 64, 1164.

39. McLaren, J. W.; Lam, J. W. *Spectrochim. Acta*, Part B, 1990, 45B, 1091.

40. Denoyer, E. R.; Fredeen, K. J.; Hager, J. W. *Anal. Chem.* 1991, 63, 445A.

41. Karanassios, V.; Horlick, G. *Spectrochim. Acta*, Part B, 1989, 44B, 1387.

42. Whittaker, P. G.; Lind, T.; Williams, J. G.; Gray, A. L. *Analyst* 1989, 114, 675.

43. Hieftje, G. M.; Norman, L. A. *Int. J Mass Spec. Ion. Proc.* 1992, 118/119, 519.

44. Hu, K.; Houk, R. S. *J. Am. Soc. Mass Spectrom.* 1993, 4, 733.

45. Ingle, J. D.; Crouch, S. R. in *Spectrochemical Analysis*, Prentice Hall, Englewood Cliffs, NJ 1988, Ch. 8, pg 235.

46. Houk, R. S. in *Handbook of the Physics and Chemistry of Rare Earths*, eds. Gschneidner, K. A., Jr., and Eyring, L., Elsevier, New York, 1990, vol. 13, Ch. 89.

CHAPTER 2. ATTENUATION OF METAL OXIDE IONS IN INDUCTIVELY COUPLED PLASMA MASS SPECTROMETRY WITH A GRAPHITE TORCH INJECTOR.

A paper published in Analytical Chemistry[1]

P. Scott Clemons, Michael G. Minnich and R. S. Houk[2]

Abstract

Desolvated solution aerosols are injected into the axial channel of an inductively coupled plasma (ICP) through a graphite tube inserted directly into the plasma. This hot injector constricts the stream of analyte and prevents it from widening excessively as it travels through the plasma. Thus, the sampling orifice for the mass spectrometer (MS) can be positioned several millimeters downstream from the tip of the initial radiation zone without substantial loss of analyte ion signal. The signal ratio for LaO^+/La^+ can be reduced to 0.05% with conventional desolvation or 0.01% with cryogenic that yield maximum metal ion signal. These values are greatly superior to those obtained with conventional torch injectors.

---

[1]*Anal. Chem.* 1995, 67, 1929-1934

[2]Corresponding author

The graphite injector also improves sensitivity for atomic ions by factors of 1.5 to 15, with the best improvements seen for elements like As and Zn that have high ionization energies. This modification to the plasma does not compromise other analytical figures of merit such as rinse out time or the suitability of a single set of operating conditions for multielement analysis.

Introduction

ICP-MS is a sensitive and selective method for trace multielement analysis. The ability of the ICP to efficiently atomize the sample is one dimension of the overall selectivity of the technique. Although atomic ions (M^+) are the major species seen under normal operating conditions, other ions such as MO^+, ArM^+, ArO^+, and Ar_2^+ hamper the determination of several important elements. Corrections based on isotope ratios can often be done for moderate cases of spectral interference,[1,2] but these procedures become suspect when the analyte signal is small relative to that for the interferant.

This paper focuses on a new method to remove most of the interference from MO^+ ions. A variety of such measures have been demonstrated for low-resolution instruments based on quadrupole mass analyzers. These schemes include mixed gas plasmas[3-8] and introduction of the sample in as dry a form as

possible, i.e., by desolvation,[4,9,10] electrothermal vaporization[11-14] or laser ablation.[1] A double focussing mass spectrometer can separate MO^+ from M^+ ions at the same nominal m/z value. In general, reducing the slit widths to attain the resolution required (6000 to 15000) also reduces the transmission by at least a factor of ten.[15,16] Measures that reduce the level of MO^+ ions in the plasma would be valuable for either low or high-resolution experiments.

The fundamental reasons for the persistence of MO^+ ions have been discussed by several groups.[17-20] Suppose an aqueous solution is dispersed into droplets with a conventional nebulizer. The larger droplets, and much of the water vapor, are then removed by a cooled spray chamber. The spray chamber still transmits wet droplets in a range of sizes to the plasma. As these droplets leave the torch injector and traverse the plasma, they are first desolvated, then the solutes are progressively vaporized, atomized and ionized. The axial positions where these processes take place overlap. The smaller droplets desolvate, vaporize, etc. relatively quickly, while the larger droplets persist much farther downstream.[21-25] Furthermore, the stream of droplets, and the resulting clouds of atoms and ions, spread out as they travel further downstream. In ICP-MS, the sampler-skimmer combination transmits ions essentially from a small zone (of approximately the same diameter as the skimmer hole) that is

just in front of the sampler.[26,27] Thus, the best sensitivity for M^+ ions generally occurs when the aerosol gas flow rate, plasma power and sampling position are selected so that the sampler tip is just downstream from the end of the initial radiation zone (IRZ).[28-32] Metal oxide ions from the larger droplets and solid particles do not pass through the middle of the normal analytical zone (NAZ), which is probably the hottest part of the axial channel.[33-36] Thus, these metal oxide ions are extracted into the sampler before they are dissociated properly, so the spectrum consists of a mixture of M^+ and MO^+.

Much of the MO^+ ions can be dissociated into M^+ by retracting the plasma farther away from the sampler or by reducing the aerosol gas flow rate. These simple measures do attenuate the MO^+ interference, but at the expense of M^+ signal.[28-32] The stream of analyte ions is now too wide at the sampler, so a larger fraction of the ions lies outside the narrow central region (~1 mm wide) transmitted through both the sampler and skimmer. At the gas kinetic temperatures prevalent in the axial channel of the ICP (~5000 K),[33,34] some MO^+ ions probably persist, particularly for refractory oxides like LaO^+ and UO^+, even if drastic measures are taken to reduce the density of O atoms in the plasma.[37]

Ideally, then, the MO^+ ions should be attenuated by a) use of a nebulizer that produces either monodisperse droplets

or polydisperse droplets without overly large ones, b) preventing the cloud of analyte from expanding as it travels through the axial channel, so the sampler can be positioned in the middle of the NAZ, rather than at the tip of the IRZ, and c) removing solvent and other sources of oxygen. The first two of these measures is incorporated in the new monodisperse dried microparticulate injection device described by French et al.[18] and Olesik and Hobbs.[19] The present work describes a way to accomplish much the same objectives using a conventional nebulizer. Essentially, a desolvated polydisperse aerosol passes through a hot graphite tube inserted directly into the axial channel of the ICP (Figure 1). This approach resembles the direct solid introduction experiments with graphite cups described by several groups,[38-40] particularly those of Horlick, Salin and Karanassios.[41-43] In most of these previous experiments, the injector is solid graphite, the sample is a solid rather than a solution aerosol, and there is no gas flow through the injection device. Gervais and Salin have described ICP emission experiments with a solution aerosol in a carrier gas passing through a heated injector (either graphite or alumina) inserted directly into the plasma. The main goal of their study was to improve the stability of the plasma with new sample introduction systems that were either erratic or loaded the plasma heavily.[44] To the best of our knowledge, this latter approach for injecting aerosols has not

been described previously for ICP-MS.

Experimental

Nebulizer and Torch Injector. Aqueous aerosols are produced with an ultrasonic nebulizer (Model U-5000, Cetac Technologies, Inc.) and desolvated by heating to 140 °C, followed by a condenser at 0 °C.[45] The resulting dry particles, and residual water vapor, then pass through a Tygon transfer tube (8 mm ID x 1 m long) connected to the end of the stainless steel tube shown at the left side of Figure 1. This tube is held on center by a tapered piece of Teflon that fits into the taper joint at the base of the torch. A pyrolytic graphite tube (2 mm ID x 5 mm OD x 22 mm long) is press fit into the end of the stainless steel support. The tip of the graphite injector protrudes into the axial channel of the plasma by approximately 8 mm. The exposed end of the injector is even with the middle turn of the load coil. Longer injectors erode too rapidly. Before use, each tip is leached in 5% HCl for 8 hours. Otherwise, a variety of metal impurity ions are observed.

In several experiments, the performance of the graphite injector shown in Figure 1 is compared to that of a conventional injector. In the latter case, the conventional injector is quartz with a tapered jet tip (1.5 mm ID) positioned even with the end of the intermediate tube.[46]

Cryogenic Desolvation. In some experiments, the aerosol is dried further by cryogenic desolvation, as described previously.[9,10] Essentially, the stream of solid particles from the condenser of the regular desolvator passes through a series of hot (140 °C) and cold (-80 °C) loops, which repeatedly dry the particles and freeze out the solvent vapor. The dry aerosol particles then go into the injector and ICP.

ICP-MS Instrumentation. These experiments were performed with a home-made ICP-MS device that has been described previously.[47,48] The offset ion lens was changed slightly in that a tapered metal cylinder was substituted for the cone (see Figure 2 of ref. 47). This arrangement yielded slightly higher ion signals with the same background as that seen previously.[47,48]

Data were collected with a multichannel analyzer by either single ion monitoring or scanning. For measurement of M^+ and MO^+ signals, a m/z window 20 daltons wide was scanned 100 times, using 4096 channels and a dwell time of 50 μs per channel. The mass analyzer was adjusted to provide unit mass resolution (5% valley) in the mass window monitored.

In general, operating conditions, particularly aerosol gas flow rate and ion lens voltages, were selected at the beginning of each day's experiments to maximize the signal for the analyte(s) of interest. Because different injectors were used on different days, these optimum conditions differed

slightly from day to day. Typical operating conditions are cited in Table I. Generally, the same power and sampling position were used from day to day, and the aerosol gas flow rate was optimized to provide maximum signal for La^+.

Solutions and Standards. Standard solutions of the elements of interest were prepared by diluting standard stock solutions (1000 mg L^{-1}, Plasma Chem) with 1% HCl to known concentrations, usually either 100 or 500 $\mu g\ L^{-1}$.

Results and Discussion

General Observations. The plasma ignites readily with the injector in place using the normal ignition procedure with a Tesla coil. The injector emits orange light during operation, which indicates that its temperature is approximately 1800 K. The appearance of the plasma is shown in color on the cover of this issue and in Figures 1 and 2. When a solution of yttrium is injected, the IRZ and NAZ[28] are roughly as depicted in Figure 1. In particular, the IRZ is very short, and the NAZ is visually longer and narrower than that seen with a conventional torch injector. A gap can clearly be seen between the blue analyte stream and the outer edge of the axial channel, i.e., the boundary between the axial channel and the induction region. When the sampling orifice is inserted at the usual sampling position (Figure 2), virtually all the blue analyte stream flows into the sampler,

even though the sampler is several mm downstream from the tip of the IRZ. With a conventional injector, the blue analyte stream is much wider and fills the entire axial channel almost immediately after the IRZ.

The injector erodes slowly during use and lasts 6 to 8 hours. The erosion occurs primarily inside the downstream tip of the injector. The hole expands gradually at the tip from a cylindrical bore to a fluted end. A fresh injector is therefore used each day. The injector is replaced easily by simply reaching into the open end of the torch with a pair of tweezers (with the plasma off, of course).

DC voltages between -100 V and +100 V can be applied to the stainless steel support tube without any noticeable change in the plasma or in the ion signal seen by the mass analyzer. Therefore, the injector is simply kept grounded.

The background spectrum is somewhat different than usual when the graphite injector is used. Carbon ions ($^{12}C^+$) are a major peak with the injector and are of comparable intensity to $^{16}O^+$, H_2O^+, and $^{40}Ar^+$. Also, CO^+ (m/z = 28) becomes more abundant than O_2^+ (m/z = 32) with the graphite injector. These and other carbon-containing ions are more abundant under conditions in which the injector erodes more rapidly. The erosion rate is, in turn, related to the type of graphite used; pyrolytic graphite erodes more slowly than spectroscopic grade graphite. The precise relation between erosion rate,

the character of the background spectrum, and the abundance of MO^+ is presently under detailed study. Deposition of solid carbon on the sampler has not been a problem so far.

MO^+/M^+ Ratios with Desolvation at 0 °C. A plot of signal for La^+ and LaO^+ vs. aerosol gas flow rate is shown in Figure 3. The best signal for La^+ is ~10^6 counts s^{-1} at an aerosol gas flow rate of ~0.6 L min^{-1}. At this value for aerosol gas flow rate, the LaO^+ signal is ~10^3 counts s^{-1}, so the ratio of signals for LaO^+/La^+ is ~0.1%. At 0.45 L min^{-1}, the La^+ signal falls off only slightly to 8 x 10^5 counts s^{-1}, whereas the LaO^+/La^+ signal ratio drops to 0.05%. This latter value is comparable to that achieved with conventional torch injectors for similar elements by drying the plasma thoroughly by cryogenic desolvation,[9,10] membrane desolvation,[49] or electrothermal vaporization.[11-14]

This result can be shown more clearly by normalizing the signals for La^+ and LaO^+ to their maxima and plotting the results on a linear scale (Figure 4). Two separate peaks (commonly called "mountains" in ICP-MS parlance) for La^+ and LaO^+ result. The peak of the mountain for La^+ lies at a much lower flow rate than that for LaO^+, by 0.3 L min^{-1}. Furthermore, the left edge of the mountain for LaO^+ is steep, and only a small amount of LaO^+ remains under the peak for La^+. With conventional torch injectors, the mountain top for M^+ lies much closer to that for MO^+, and the left edge of the MO^+

mountain has a much more gradual slope than that shown in Figure 4. Thus, a substantial amount of MO^+ remains under conditions that maximize M^+ signal, for the reasons described in the Introduction.

At the "best" aerosol gas flow rate in Figures 3 and 4 (0.6 L min^{-1}), the relative positions of the IRZ and sampling orifice are those shown in Figure 2. With the graphite torch injector, the sampler can be 4 to 5 mm downstream from the tip of the IRZ without substantial loss of signal for M^+. In contrast, with conventional torch injectors, the maximum M^+ signal is generally obtained with the sampler only ~1 mm downstream from the tip of the IRZ, which complicates selection of operating conditions that maximize sensitivity for M^+ while also minimizing the abundance of MO^+.[30-32]

MO^+/M^+ Ratios with Cryogenic Desolvation. Figure 5 shows the dependence of La^+ and LaO^+ signals on aerosol gas flow rate with cryogenic desolvation and the graphite torch injector. Within the flow rate range from 0.4 to 0.8 L min^{-1}, the La^+ signal is a maximum while the LaO^+/La^+ signal ratio is only 0.01% to 0.02%. This represents roughly a five-fold improvement in LaO^+/La^+ over the oxide ratio obtained by either regular desolvation with the graphite torch injector or cryogenic desolvation with a conventional torch injector.[9,10]

Unfortunately, the La^+ signal is reduced by cryogenic desolvation with either the graphite injector or a

conventional one.[9,10] With the graphite injector, adding H_2 gas at 2% of the aerosol gas flow boosts the M^+ signal by approximately a factor of two. This signal enhancement is slightly poorer than the factor of three seen previously.[10] Adding H_2 through the graphite torch injector also increases the oxide ratio for LaO^+/La^+ by a factor of four, so use of H_2 has not proven advantageous so far.

Multielement Operating Conditions. Ideally, the signal from all analytes should be nearly optimum at a single set of operating conditions. The constriction of the analyte stream induced by the graphite injector could also induce substantial differences in the "best" plasma parameters for different elements, which was a problem for the long torches used in some early ICP-MS devices[29] and in atomic fluorescence with the ICP.[50]

Ion signals for a variety of elements are shown as functions of aerosol gas flow rate in Figure 6. For all these elements, the M^+ signal is at or within 10% of its maximum value at a single setting for aerosol gas flow rate (0.45 L min^{-1}). This value is lower than the "best" value of 0.6 L min^{-1} from the previous figures because this experiment was done on a different day with a fresh injector. Each injector behaves slightly differently and requires a somewhat different aerosol gas flow rate to provide optimum M^+ signal and to minimize oxide ions.

Analogous results are seen if forward power and sampling position are varied. These operating conditions are all interrelated, as pointed out by Horlick and co-workers.[29-32] To a first approximation, an increase in power requires an increase in aerosol gas flow rate and/or positioning the sampler further upstream in the plasma.

Sensitivity Improvements. For these experiments, sensitivity is defined as net ion signal per unit concentration. These values are compared in Table II. The results for both the graphite injector and the conventional injector were obtained with the same power and sampling position. In each case, the aerosol gas flow rate was adjusted to maximize La^+ signal. Thus, the sensitivities provided by the two injectors are compared under conditions of best sensitivity for each. Also, each injector was operated under multielement conditions; conditions were not optimized separately for individual elements.

With the conventional injector, sensitivities are in the range 10^5 - 10^6 counts s^{-1} per mg L^{-1}, as seen previously with this particular ICP-MS device.[47,48] For every element, these values improve with the graphite injector. Sensitivities for Fe, Ho and Pb improve by factors of 1.5 to 1.8. The graphite injector improves the sensitivity for other elements by larger factors ranging from 5 (for Y, Mo and Rh) to 10 - 15 for Zn and As.

These element-dependent sensitivity improvements can be explained as follows. The injector constricts the stream of analyte ions somewhat for all elements, as depicted in Figures 1 and 2. A larger fraction of the analyte ions stays on-axis within the zone of gas that passes through both the sampler and skimmer. Thus, sensitivity improves somewhat for all elements, even those like Fe and Y that are almost completely ionized in the normal ICP. Also, the graphite injector allows the sampling orifice to be positioned near the middle of the NAZ where the "temperature" for analytes is highest.[33-36] Of the various elements studied, this change in sampling position improves the degree of ionization most for elements like As and Zn, which aren't efficiently ionized at the tip of the IRZ in a normal ICP. Thus, the sensitivity for As and Zn improves by larger factors than those seen for more easily ionized elements.

The sensitivity improvements seen in Table II are welcome even if their fundamental causes are not yet fully understood. Because these improvements result from a change in the structure of the plasma, they should be useful with other ICP-MS devices as well.

Rinse Out Curves. Conceivably, injecting the sample aerosol through a hot graphite tube could induce additional memory problems and extend the time needed to change samples. A typical rinse out curve is presented in Figure 7. The Cd

solution is replaced with the blank solution at time = zero. The blank reaches the transducer at time = 10 s, after which the Cd^+ signal decays gradually. After an additional 30 s, the Cd^+ signal reaches 0.1% of its original level. After 55 s, the Cd^+ signal can't be distinguished from the blank.

This rinse-out behavior (i.e., 30 s to attenuate the signal from the previous sample by 0.1%) is identical to that of the nebulizer alone. Similar curves are seen for a variety of other elements, including Zn and Co. For these elements, the graphite injector induces no additional memory. Naturally, severe memory effects occur for highly volatile elements like B, Os and Hg, as generally seen whenever the aerosol passes through a spray chamber.[45] We have not yet tested the graphite injector extensively with wet aerosols.

Conclusions

The graphite injector described in this paper provides a simple way to extract M^+ ions from a region of the plasma that is physically separated from the zone inhabited by the noxious MO^+ ions. Signal ratios for MO^+/M^+ can be reduced to 0.01% to 0.05% by this means. Analyte sensitivity can be improved by factors of 1.5 to 15. The basic reasons for these improvements are being investigated further in our laboratory, as are other analytical characteristics such as matrix effects.

Acknowledgement

Ames Laboratory is operated for the U. S. Department of Energy by Iowa State University under Contract No. W-7405-Eng-82. This research was supported by the Office of Basic Energy Sciences. The graphite tubes were provided gratis by Union Carbide.

References

1. Jarvis, K. E.; Gray, A. L.; Houk, R. S. *Handbook of ICP-MS*, Blackie: London, 1992, Chaps. 4.2 and 10.3.
2. Date, A. R.; Cheung, Y. Y.; Stuart, M. E. *Spectrochim. Acta*, Part B 1987, 42B, 3.
3. Lam, J. W. H.; Horlick, G. *Spectrochim. Acta*, Part B 1990, 45B, 1313.
4. Lam, J. W. H.; McLaren, J. W. *J. Anal. Atomic Spectrom.* 1990, 5, 419.
5. Louie, H.; Soo, S. Y.-P. *J. Anal. Atomic Spectrom.* 1992, 7, 557.
6. Evans, E. H.; Ebdon, L. *J. Anal. Atomic Spectrom.* 1990, 5, 425.
7. Wang, J.; Evans, E. H.; Caruso, J. A. *J. Anal. Atomic Spectrom.* 1992, 7, 929.
8. Laborda, F.; Baxter, M. J.; Crews, H. M.; Dennis, J. *J. Anal. Atomic Spectrom.* 1994, 9, 727-736.

9. Alves, L. C.; Wiederin, D. R.; Houk, R. S. *Anal. Chem.* 1992, 64, 1164.

10. Alves, L. C.; Allen, L. A.; Houk, R. S. *Anal. Chem.* 1993, 65, 2468.

11. Gregoire, D. C. *J. Anal. Atomic Spectrom.* 1988, 3, 309.

12. Shibata, N.; Fudagawa, N.; Kubota, N. *Spectrochim. Acta,* Part B, 1992, 47B, 505; 1993, 48B, 1127.

13. Gregoire, D. C.; Sturgeon, R. E. *Spectrochim. Acta,* Part B, 1993, 48B, 1347.

14. Ediger, R. D.; Beres, S. A. *Spectrochim. Acta,* Part B 1992, 47B, 907.

15. Bradshaw, N.; Hall, E. F. H.; Sanderson, N. E. *J. Anal. Atomic Spectrom.* 1989, 4, 801.

16. Morita, M.; Ito, H.; Uehiro, T.; Otsuka, K. *Anal. Sci.* 1989, 5, 609.

17. Tanner, S. D. *J. Anal. Atomic Spectrom.* 1993, 8, 891.

18. French, J. B.; Etkin, B.; Jong, R. *Anal. Chem.* 1994, 66, 685.

19. Olesik, J. W.; Hobbs, S. E. *Anal. Chem.* 1994, 66, 3371.

20. Vanhaecke, F.; Dams, R.; Vandecasteele, C. *J. Anal. Atomic Spectrom.* 1993, 8, 433.

21. Olesik, J. W.; Smith, J. J.; Williamsen, E. *J. Anal. Chem.* 1989, 61, 2002.

22. Olesik, J. W.; Fister, J. C., III *Spectrochim. Acta,* Part B 1991, 46B, 869.

23. Cicerone, M. T.; Farnsworth, P. B. *Spectrochim. Acta*, Part B 1989, 44B, 897.

24. Winge, R. K.; Crain, J. S.; Houk, R. S. *J. Anal. Atomic Spectrom.* 1991, 6, 601.

25. Winge, R. K.; Chen, X.; Houk, R. S. *J. Anal. Atomic Spectrom.* 1995, 10, in preparation.

26. Douglas, D. J.; French, J. B. J. Anal. Atomic Spectrom. 1988, 3, 743.

27. Douglas, D. J. Fundamental Aspects of ICP-MS, in *ICPs in Analytical Atomic Spectrometry*, 2nd ed., Montaser, A.; Golightly, D. W., Eds., VCH: New York, 1992, Chap. 13.

28. Koirtyohann, S. R.; Jones, J. S.; Yates, D. A. *Anal. Chem.* 1980, 52, 1965.

29. Horlick, G.; Tan, S. H.; Vaughan, M. A.; Rose, C. A. *Spectrochim. Acta*, Part B, 1985, 40B, 1555.

30. Tan, S. H.; Horlick, G. *J. Anal. Atomic Spectrom.* 1987, 2, 745.

31. Vaughan, M. A.; Horlick, G. *Appl. Spectrosc.* 1986, 40, 434.

32. Horlick, G.; Shao, Y. ICP-MS for Elemental Analysis, in *ICPs in Analytical Atomic Spectrometry*, 2nd ed., Montaser, A.; Golightly D. W., Eds., VCH: New York, 1992, Chap. 12.

33. Hasegawa, T.; Umemoto, M.; Haraguchi, H.; Hsiech, C.; Montaser, A., in *ICPs in Analytical Atomic Spectrometry*, 2nd ed., Montaser, A.; Golightly, D. W., Eds., VCH: New York, 1992, Chap. 8.

34. Hanselman, D. S.; Sesi, N. N.; Huang, M.; Hieftje, G. M. *Spectrochim. Acta*, Part B, 1994, 49B, 495.

35. Furuta, N.; Horlick, G. *Spectrochim. Acta*, Part B, 1982, 37B, 53.

36. Houk, R. S.; Olivares, J. A. *Spectrochim. Acta*, Part B, 1984, 39B, 575.

37. Nonose, N. S.; Matsuda, N.; Fudagawa, N.; Kubota, M. *Spectrochim. Acta*, Part B, 1994, 49B, 955.

38. Sommer, D.; Ohls, K. *Fresenius Z. Anal. Chem.* 1980, 304, 97.

39. Zaray, G.; Broekaert, J. A. C.; Leis, F. *Spectrochim. Acta*, Part B, 1988, 43B, 241.

40. Kirkbright, G. F.; Li-Xing, Z. *Analyst* 1982, 107, 617.

41. Salin, G. D.; Horlick, G. *Anal. Chem.* 1979, 51, 2284.

42. Karanassios, V. K.; Horlick, G.; Abdullah, M. *Spectrochim. Acta*, Part B, 1990, 45B, 105.

43. Boomer, D. W.; Powell, M.; Sing, R. L. A.; Salin, E. D. *Anal. Chem.* 1986, 58, 975.

44. Gervais, L. S.; Salin, E. D. *J. Anal. At. Spectrom.* 1991, 6, 493.

45. Bear, B. R.; Fassel, V. A. *Spectrochim. Acta*, Part B, 1986, 41, 1089.

46. Scott, R. H.; Fassel, V. A.; Kniseley, R. N.; Nixon, D. E. *Anal. Chem.* 1974, 46, 75.

47. Hu, K.; Clemons, P. S.; Houk, R. S. *J. Amer. Soc. Mass Spectrom.* 1993, 4, 16.

48. Hu, K.; Houk, R. S. *J. Amer. Soc. Mass Spectrom.* 1993, 4, 28.

49. Zhu, J. J.; Smith, F. G. Federation of Anal Chem. and Spectrosc. Socs. Mtg., St. Louis, MO, October 1994, Paper No. 780.

50. Demers, D. R.; Montaser, A. *ICPs in Analytical Atomic Spectrometry*, 2nd ed., Montaser, A.; Golightly, D. W., Eds., VCH: New York, 1992, Chap. 11.

Table 1. Standard operating conditions

Solution uptake rate	1.5 mL min^{-1}
Argon gas flow rates:	
outer gas	16 L min^{-1}
auxiliary	0.9 L min^{-1}
aerosol gas	0.4 to 0.6 L $min^{-1,a}$
Forward power	1.5 kW
Reflected power	< 5 W
Sampling position	5 mm from load coil
	on center
	see Figure 2

[a]Selected on daily basis to maximize signal for La^{+}

Table 2. Relative sensitivity for various elements with conventional injector and graphite injector.

Element	Ionization Energy (eV)	Sensitivity x10^5 (cts s^{-1}/mg L^{-1}) Conv. Injector	Graphite Injector	Sens. Ratio
^{56}Fe	7.87	2.28	3.42	1.5
^{59}Co	7.86	1.88	6.34	3.4
^{64}Zn	9.39	4.53	6.64	15
^{75}As	9.81	1.15	1.69	14.6
^{89}Y	6.38	1.00	5.28	5.3
^{98}Mo	7.10	2.05	1.16	5.7
^{103}Rh	7.46	6.62	4.02	6.0
^{165}Ho	6.02	4.42	7.98	1.8
^{208}Pb	7.42	9.32	1.52	1.6

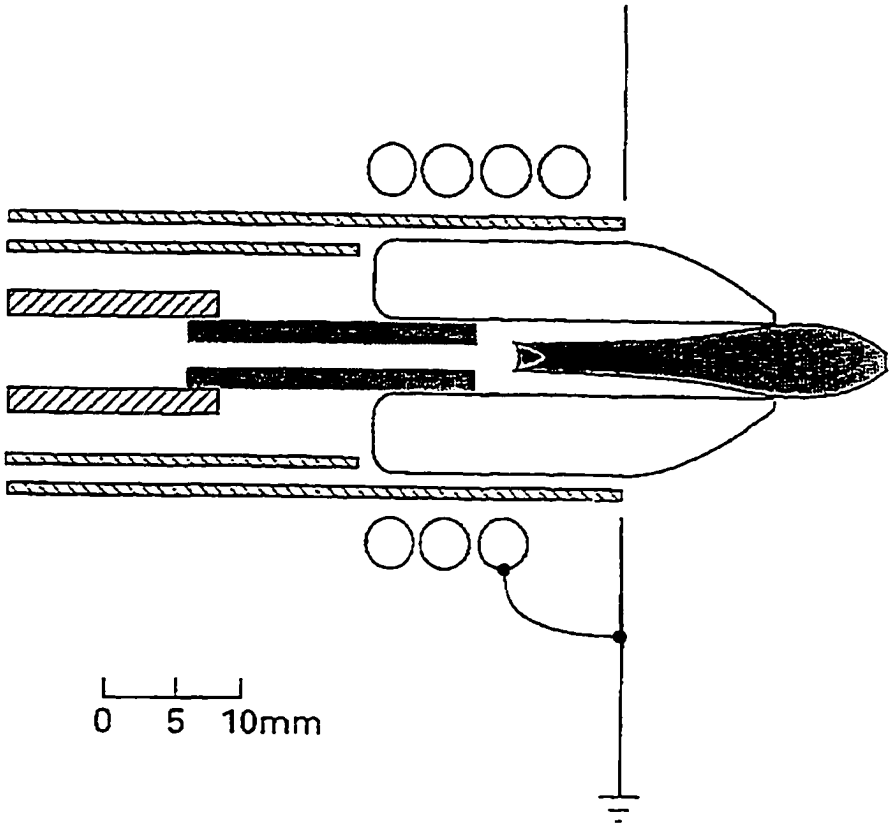

Figure 1. Diagram of an ICP with graphite torch injector. A: desolvated aerosol from ultrasonic nebulizer; B: stainless steel support tube; C: graphite injector; D: initial radiation zone (IRZ); E: normal analytical zone (NAZ). The sizes and positions of the IRZ and NAZ are shown to scale when a concentrated solution (~1000 mg L^{-1}) of yttrium is nebulized.

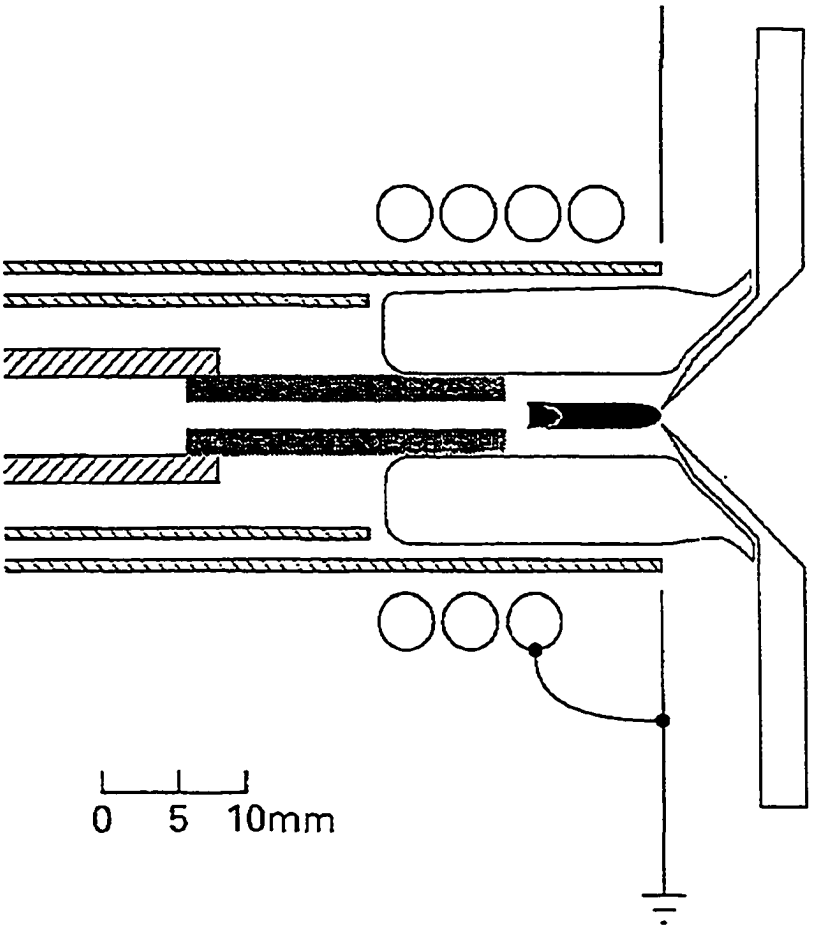

Figure 2. ICP with graphite torch injector from Figure 1 with sampling orifice of MS present at usual sampling position. Not that viurtually all the analyte ions flow into the sampling orifice.

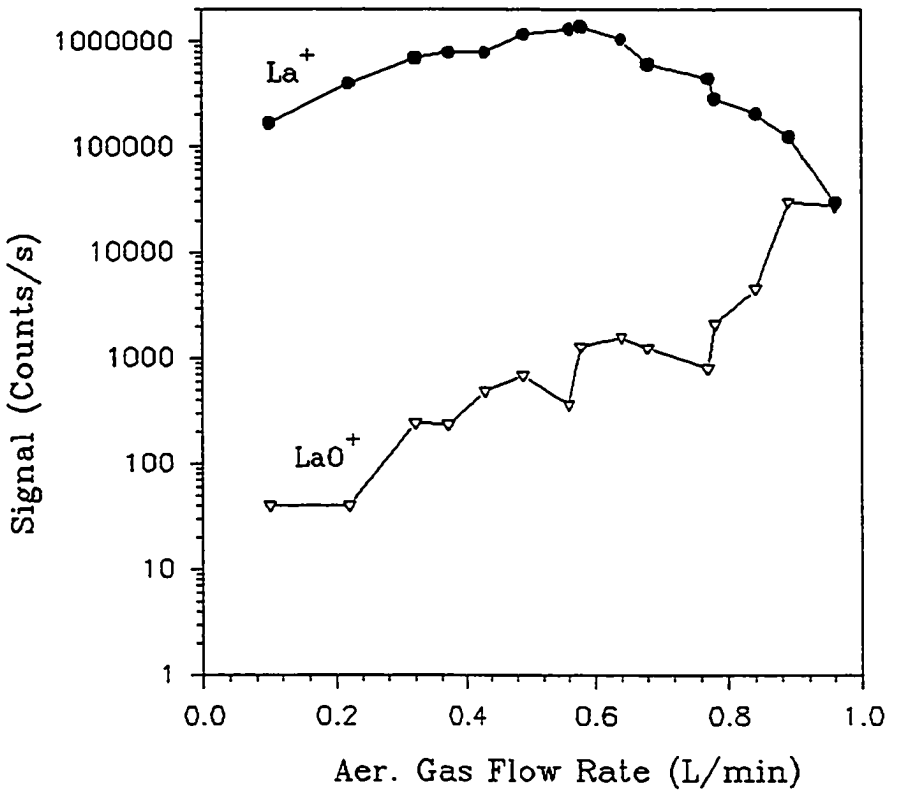

Figure 3. Plots of ion signal vs. aerosol gas flow rate for La+ and LaO+ with graphite injector and conventional desolvation.

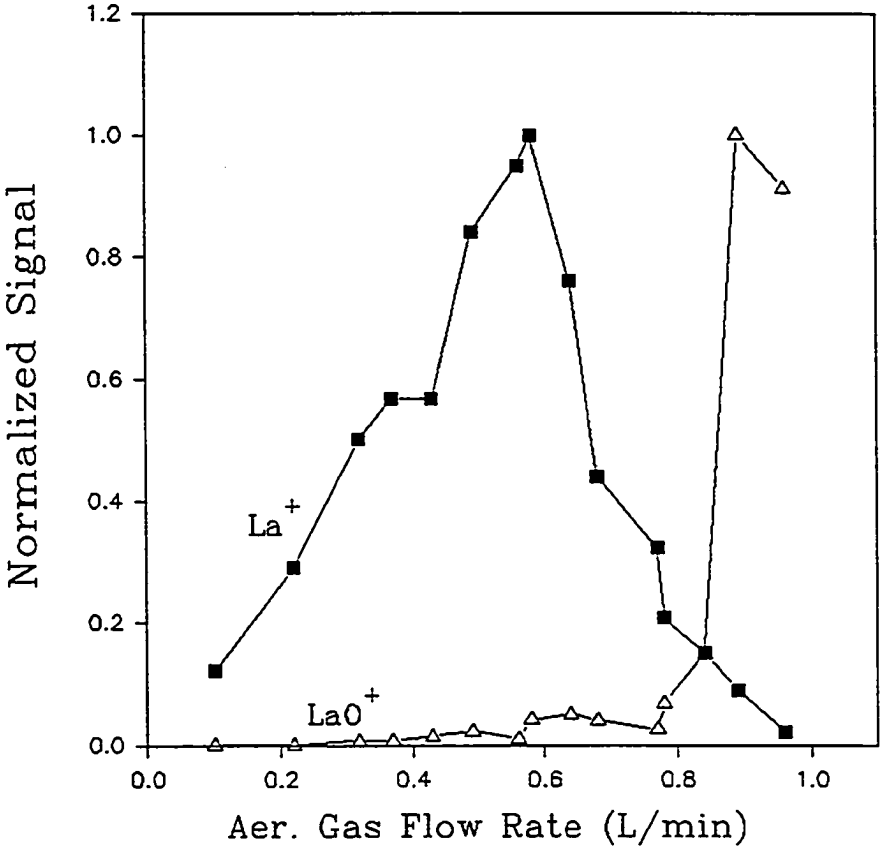

Figure 4. Plots of normalized ion signals for La+ and LaO+ vs. aerosol gas flow rate, conventional desolvation.

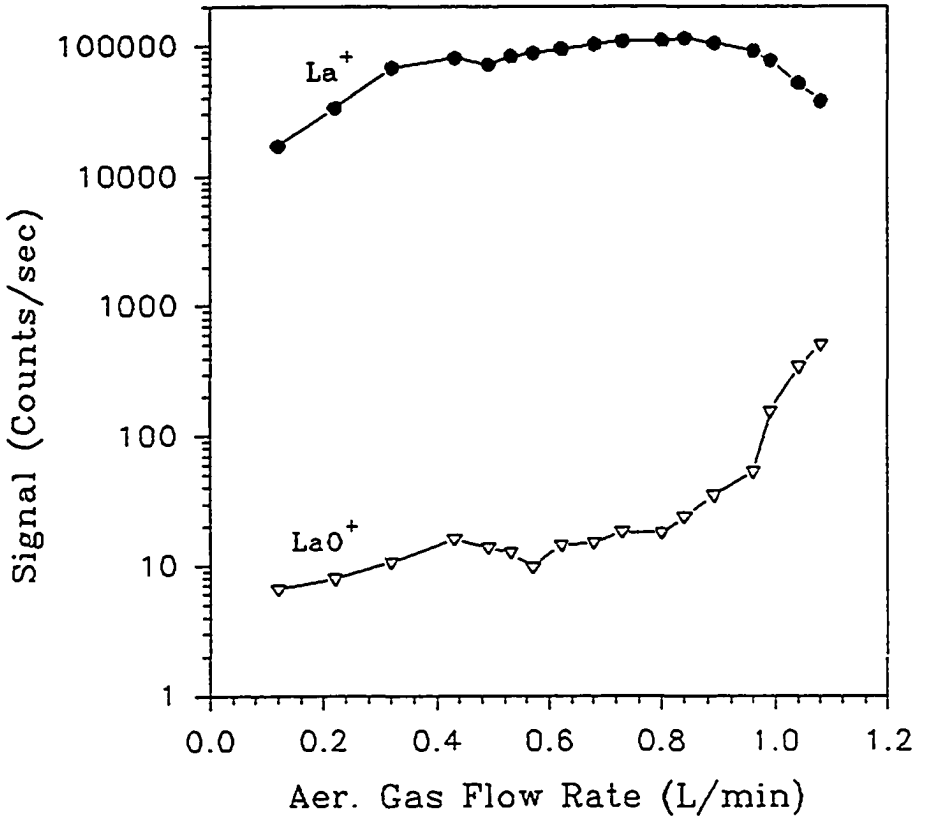

Figure 5. Ion signals vs. aerosol gas flow rate with cryogenic desolvation.

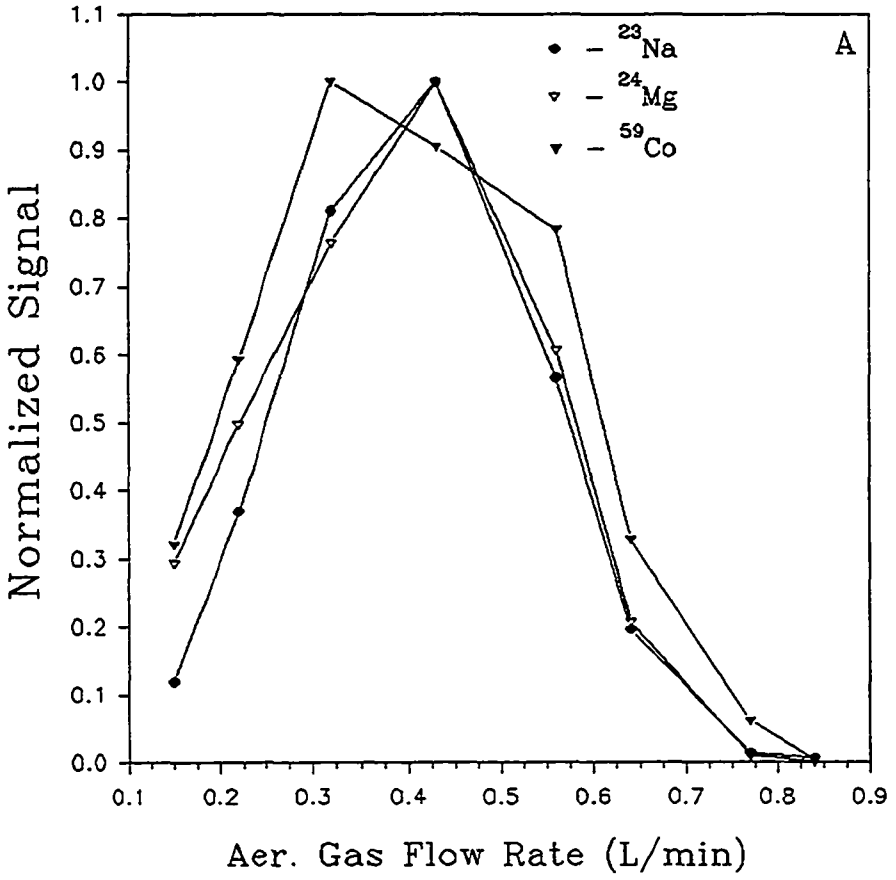

Figure 6. Normalized signal for M^+ vs. aerosol gas flow rate for some common analyte elements, each at 100 ug L^{-1}.

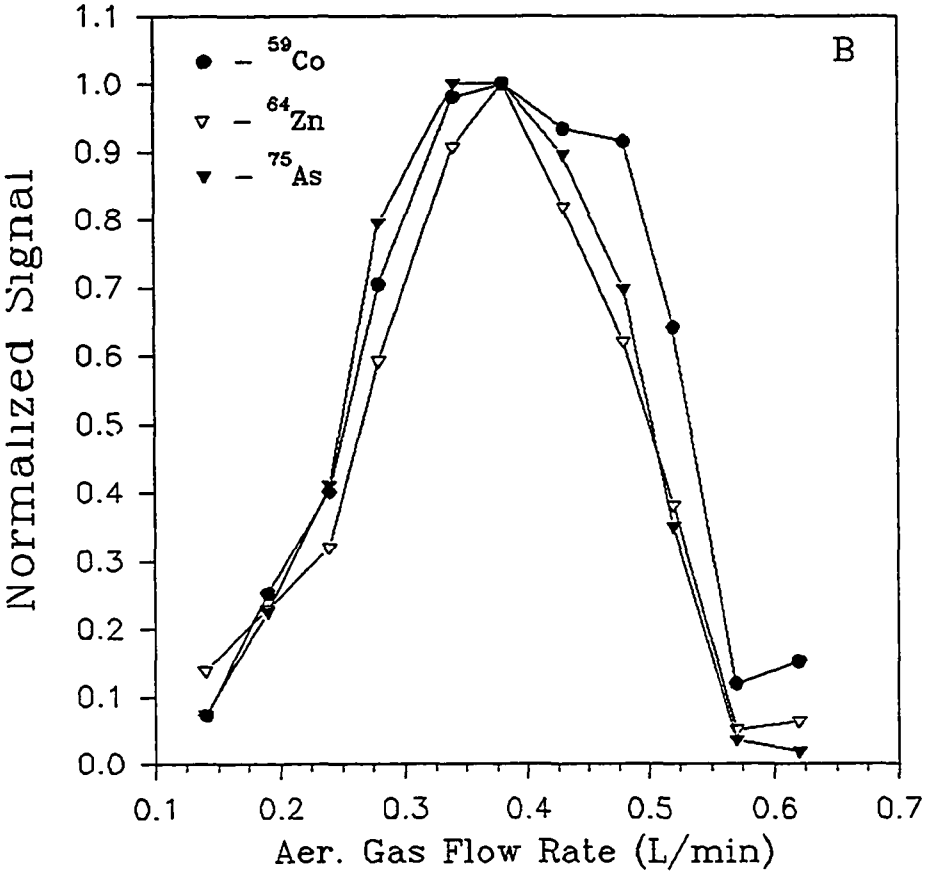

Fig. 6 (continued)

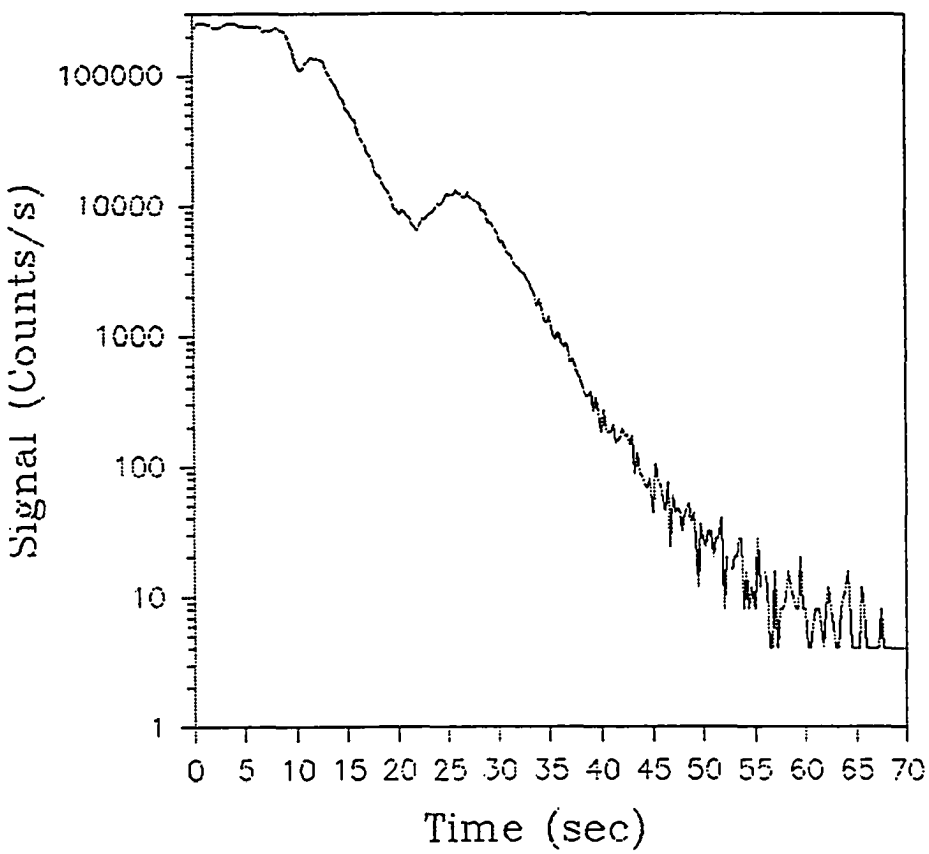

Figure 7. Rinse-out curve for Cd at 1 mg L^{-1}. The rinse solution reaches the transducer of the nebulizer at about time = 10 s.

CHAPTER 3. BACKGROUND IONS, SPECTRAL INTERFERENCES AND MATRIX EFFECTS IN INDUCTIVELY COUPLED PLASMA MASS SPECTROMETRY WITH A GRAPHITE TORCH INJECTOR

A paper submitted for publication to Spectrochimica Acta, Part B, Atomic Spectroscopy

P. Scott Clemons, Narong Praphairaksit, and R.S. Houk[1]

Abstract

The background ions produced during the use of a graphite injector (GI) and inductively coupled plasma mass spectrometry (ICP-MS)are evaluated. A spectrum of low mass background ions reveals that C^+, CO^+ and CO_2^+ are a result of using this device. Background equivalent concentration (BEC) values are presented for less abundant polyatomic ions in the mid-mass region. The BEC value for $^{35}Cl^{16}O^+$ and $^{40}Ar^{35}Cl^+$ is about ten times lower with the GI than with a conventional quartz injector (QI). The carbon load to the plasma resulting from the eroding graphite produces $^{40}Ar^{12}C^+$ with a BEC of 12 ug L^{-1}. Iron background ions from a stainless steel support tube are largely removed by using an alumina tube. Despite this change the BEC value for $^{40}Ar^{16}O^+$ is two times greater with a GI. Doubly

---

[1]Corresponding author

charged ions are more abundant for elements with a low second ionization energy. Matrix effects are evaluated and found to be equivalent to those observed previously with this device. Lens elements are tuned to mitigate this problem.

Introduction

Recently, a new injector device was introduced that boosts analyte signals and attenuates metal oxide ions in inductively coupled plasma mass spectrometry (ICP-MS).[1] These initial experiments focused on the reduction of metal oxides, but other types of spectral interferences exist in ICP-MS. Interferences from species derived from argon, mineral acids and doubly charged analyte or matrix ions are also troublesome, in addition to metal oxide ions. Lists of these interferences have been compiled and will not be duplicated here.[2-5]

Many authors have developed ingenious ways to suppress these troublesome ions in quadrupole ICP-MS. Hard core solvent removal such as cryogenic desolvation works well for metal oxides and some mineral acid polyatomics, but this method suffers from signal loss unless aided by addition of hydrogen.[6] Introduction of the sample as a solid can eliminate the polyatomic ions from the usual solvents. Laser ablation, electrothermal vaporization and direct sample insertion have all been tried and found to be useful in

certain applications.[7-9] The transient signals resulting from these methods are not conducive to peak hopping during multielemental determinations.[10] Also, counting statistics can limit the relative standard deviation as the signal cannot be integrated for a long period. Others have produced mixed gas plasmas by addition to the outer gas (N_2,O_2, or air),[11-13] and small doses (a few percent Xe, or molecular gas) to the aerosol gas with some success.[14,15] More recently, the use of a "cool" plasma to avoid interferences with higher ionization energies has been tried.[16,17] Many argon interferences were eliminated but other polyatomic ions, such as NO^+,H_3O^+ and O_2^+, became worse.

This paper investigates the level of certain common polyatomic ions and doubly charged metal ions during use of a graphite injector tip. Major background ions are presented in spectra. Minor, yet troublesome, polyatomic ions are evaluated with the measurement of background equivalent concentration (BEC) values. Finally, the severity of matrix effects while using this device will be investigated. A method for alleviating this type of interference is included.

Experimental

Dimensions and details of the operation of this device have been discussed previously, and all experiments were carried out on the same homemade ICP-MS instrument described

before.[1,18,19] Operating conditions were selected daily to maximize the analyte signal of interest. Ion lens potential, aerosol gas flow rate, and sampling position were all adjusted to maximize an analyte ion signal near the middle of the mass range of interest, e.g., $^{59}Co^{+}$.

Graphite Tip and Injector Tube. Previous work used pyrolytic graphite (PG) as an injector tip. All the data presented here are from a spectroscopic graphite tip (SG). Our observations show that SG erodes faster in an operating plasma than PG. Even so, SG is readily available in bulk and is much easier to machine than bulk PG. Using spectroscopic graphite should give a worst case scenario for carbon related background ions in a spectrum. The particular pieces used were of the rod and cup from a DC arc electrode. The cup was simply cut off and then the correct diameter hole (2mm) was drilled thru the center for the sample to pass into the plasma. After drilling, the pieces were leached in 5% aqueous HCl as described before.[1]

A stainless steel tube was used previously to support the graphite tip.[1] Experience has shown that this material is a poor choice as it produces background Fe^{+} in the spectrum. Therefore, an alumina tube was used instead. The length (30.5 cm), outside diameter (6.50 mm) and inside diameter of the alumina tube are similar to those of the previous stainless steel support tube.

Data Acquisition. The ion signal from the Channeltron electron multiplier was processed in one of two ways. The first method was used to reduce the risk of counting loss due to high level background ions, particularly in the low mass range (m/z of 10-38). The output from the electron multiplier (-2kV) was fed to a current-to-frequency converter (Model 151, Analog Technologies Inc.). TTL pulses from the converter were counted by a multichannel analyzer. The spectrum at low m/z values was acquired by sweeping all 4096 channels of the analyzer 200 times.

All other spectra, tabled data and graphs were obtained by pulse counting. A preamplifier and amplifier-discriminator (Model 1763 and Model 1762 respectively, Photochemical Research Associates) were used in place of the converter device with the electron multiplier held at -3.0 kV. In the pulse counting mode spectra were obtained by collecting 100-500 sweeps over the mass range shown in the spectra. Regardless of how the signal was collected, a dwell time of 50 μs/address and single unit mass resolution (10% valley, or better) was used.

Solutions. Standard solutions of the elements of interest were made by diluting stock solutions (1000 mg L^{-1}, Plasma Chem). The solvents were distilled deionized water (18 MΩ, Barnstead) or 1% aqueous solutions of HCl or HNO_3. The particular acid was selected to maximize conditions for

production of the polyatomic interferant. Analyte concentrations for the solutions used to measure BEC values were 0.1 mg L^{-1}. Matrix effect experiments used 1 mg L^{-1} cobalt as the analyte concentration and 10 mM as the concomitant matrix concentration. The mass spectrum of each matrix solution was scanned prior to adding the analyte to ensure the mass to charge ratio of interest showed no signal contribution from trace analyte.

Results and Discussion

Background Ion Spectrum. ICP-MS devices produce some dominant ions in the low to mid mass region of the mass spectrum. Figures 1 and 2 show mass spectra for a m/z range of 10 to 38 and 42 to 81, respectively. The mass range of 39 to 41 was omitted to spare the detector from bombardment with argon ions. For Figure 1, a graphite tip with an alumina support tube and deionized water as the solvent are used. Most of the peaks present are expected and typical of this mass region[3]. The unusual peaks are at m/z= 12 and 28. The signal at m/z= 12 is C^+ that sublime from the injector and then ionize in the plasma. This certainly prevents determination of carbon but a worse problem would be the formation of carbide species in the form of MC^+. This possible problem will be addressed in a later section. Another peak of interest in Fig. 1 is at m/z= 28. Usually

most of the ions at this mass are $^{14}N_2^+$. As shown previously,[3] the signal at m/z= 14, $^{14}N^+$, is usually greater than the signal at m/z= 28, $^{14}N_2^+$. A best guess for the ion responsible for the increase in signal at this suspect mass is carbon monoxide, $^{12}C^{16}O^+$. The inset spectrum shows that the peak at m/z= 32, $^{16}O_2^+$, is much lower than that in a typical ICP-MS background spectrum.[3] This result may indicate how this injector device works but will not be discussed here.

Before leaving this section of the spectrum it is important to illustrate a possible, yet avoidable, drawback to this device. The small peak at m/z= 23 is probably sodium ions, $^{23}Na^+$. A major advantage to using an ICP is that it is an electrodeless discharge.[20] By placing a carbon electrode into the plasma it opens the door to interferences from contaminants in the graphite. The tip used for obtaining Fig.1 was handled with unprotected hands before being used to illustrate the necessity of having a clean graphite source for this type of experiment. Many companies produce a "spectroscopically" pure grade of graphite and this is recommended for this type of work.

Figure 2 was obtained with the same sample introduction conditions as Fig.1. A very large peak at m/z= 44 is probably $^{12}C^{16}O_2^+$. This peak is more abundant than usual.[19] Another common ion in this mass range is the argon dimer, Ar_2^+, m/z= 80. It is true that this ion is about twice as abundant as in

ref.19 but the signal CO_2^+/Ar_2^+ (m/z= 44 and 80) is overwhelmingly greater in this work. This, again, is a possible clue to how this device produces its unusual properties and will be investigated in a future endeavor. The peak at m/z= 52 is predominantly due to $^{40}Ar^{12}C^+$. The inset spectrum reveals that copper, at m/z= 63 and 65, is present, as has been seen before.[39] Isotopes of zinc, m/z= 64, 66 and 68, are present due to memory in the spray chamber as well as arsenic at m/z= 75.

Background Equivalent Concentrations. Some of the weaker peaks in Fig.2 are best described using a background equivalent concentration (BEC) value. This value is defined as the analyte concentration necessary to produce a net signal equivalent to that of the interfering ion at a given mass to charge ratio. Five common problematic polyatomic ions were chosen. As described briefly in the Experimental section, the solvent media are selected to maximize the formation of most of these ions. The ions at m/z= 51 and 75, $^{35}Cl^{16}O^+$ and $^{40}Ar^{35}Cl^+$ respectively, were measured while nebulizing 1% HCl. Argon species at m/z= 54 and 56, $^{40}Ar^{14}N^+$ and $^{40}Ar^{16}O^+$, are observed while nebulizing 1% HNO_3. The final species, $^{40}Ar^{12}C^+$, is measured while nebulizing distilled deionized water. Table 1 is a collection of the results for this experiment. Both analyte signals and BEC values are reported. The analyte signal reported reflects only the net ion signal from the

element of interest; polyatomic contributions are subtracted prior to calculating the BEC values.

Obviously, both BEC values for ClO^+ and $ArCl^+$ are reduced by a factor of about ten compared to those obtained with the quartz injector. In both these cases the analyte signals are enhanced and the chlorine containing polyatomic species are attenuated. This type of behavior has been observed before but under slightly different conditions.[21] That experiment introduced carbon into the plasma from a nebulized organic solvent. In this experiment carbon sublimes directly into the plasma, so changing the carbon load does not affect the characteristics of the aerosol produced by the nebulizer.

The polyatomic ions that interfere with the determination of iron appear to behave differently. The graphite injector enhanced the $^{54}Fe^+$ signal by a factor of 2 over that obtained with the quartz injector. The BEC value for the corresponding interference, $^{40}Ar^{14}N^+$, is two times lower using the GI. Thus, the absolute intensity of $^{40}Ar^{14}N^+$ is similar using either injector. Unfortunately for $^{56}Fe^+$, there is an increase in BEC value of about two times when using the GI over the NI. The tragedy of this polyatomic ion ($^{40}Ar^{16}O^+$) is that the absolute signal intensity is about 5 times higher. This particular polyatomic oxide ion does not behave like the metal oxide ions. This could be Fe^+ from the graphite. Especially since the injector was machined and drilled with steel.

The poorest BEC value in Table 1 is for $^{40}Ar^{12}C^{+}$. This is most certainly the worst spectral interference created by this device in this analytical region of the spectrum. The BEC value is about ten times larger than that of the normal quartz injector. Determining chromium with $^{52}Cr^{+}$ is certainly out of the question. If carbon is present in the sample or solvent, m/z= 52 cannot be used anyway. The next most abundant isotope of chromium is ^{53}Cr (9.6%). Unfortunately, $^{37}Cl^{16}O^{+}$ would interfere but not as severely as with a normal quartz injector. The next available isotope is ^{50}Cr at 4.3% relative abundance. This is a reasonable choice as long as the matrix does not include Ti or V, ^{50}Ti (5.4%) and ^{50}V(0.25%). Also, if sulfuric acid is used $^{50}Cr^{+}$ would be interfered by $^{34}S^{16}O^{+}$. In light of this information, chromium can only be determined at relatively high concentrations (> 1 ppb).

Conceivably, carbon could form charged polyatomic species with matrix elements. Experience from graphite furnace atomic absorption shows that WC is one of the worst refractory neutral carbides, and WC^{+} could thus be a problem in ICP-MS. Figure 3 is a spectrum from m/z= 186 to 205. A solution of 50 $\mu g\ L^{-1}$ thallium and 50 mg L^{-1} tungsten was made with deionized water. The second major isotope of tungsten, $^{186}W^{+}$ (28.4%), is at the left edge of the spectrum and the largest isotope of thallium, $^{205}Tl^{+}$ (70.5%), is at the far right. Using the singly charged isotope of thallium at m/z= 203 as a reference the

level of WC^+ can be assessed. The visible peaks of WO^+ from m/z= 198 to 202 are significant giving a signal of about 700 counts s^{-1}. The weak peaks shown in the inset of Fig. 3 are presumably from WC^+ and are only about 50 to 100 count s^{-1}. When compared to the signal for thallium at 50 $\mu g\ L^{-1}$ this type of interference is almost negligible and would certainly cause only a minor interference when trying to determine an element such as platinum.

Doubly Charged Ions. In the previous report, a suggestion was made for the improvements observed in analyte signal over a conventional torch arrangement.[1] The graphite injector allows the sampling orifice to be positioned in a region of the normal analytical zone where the "temperature" for the analytes is highest.[22-25] Using this as a premise, the levels of doubly charged analyte ions (M^{2+}) observed while using a graphite injector should be greater than when using a conventional quartz injector. This hurts an analysis in two ways. First, creation of additional doubly charged analyte ions sacrifices some M^+ signal. The next, more important issue, is that M^{2+} ions interfere with the determination of other lower mass elements.

Tables 2 and 3 give relative and absolute values of doubly charged ions, respectively. The elements of interest are arranged according to the magnitude of their second ionization energy (IE'). The relative count rates of M^{2+} in

Table 3 are compared to those for M^+ ions from either the same element or an internal standard close in mass to M^{+2}, to reduce mass discrimination. Also, the internal standard was chosen with a high enough IE' as to minimize its formation of M^{2+}. For the elements barium through niobium a 0.1 mg L^{-1} internal spike of cobalt was used. Lead, being much higher in mass, got a 0.1 mg L^{-1} spike of silver, and the $^{107}Ag^+$ isotope was monitored. The M^{2+} signal for multi-isotopic elements was collected by integrating all isotopes of the element, both singly and doubly charged. This was done since resolution with this device is too poor to separate adjacent peaks of doubly charged ions.

Table 2 shows that the absolute level M^{2+} is greater for the graphite injector in every case from barium to lead. As would be expected, the absolute count rate drops off steadily for both injector cases as IE' increases. Upon closer inspection it is apparent that the decrease in M^{2+} intensity with respect to increasing IE' is greater for the graphite injector than for quartz injector. Table 3 illustrates this latter point better. Generally, relative values of M^{2+} are much greater with the graphite injector for elements with an IE' of about 10 to 14 eV. For lead, with an IE' of about 15 eV, there is little difference in either of the relative values. Figure 4 is a spectrum taken with a graphite injector using 1 mg L^{-1} Pb and a 50 ug L^{-1} Nb reference. The inset

spectrum was necessary to display the unresolved Pb^{2+} isotopes. Actually, the M^{2+} level of lead is less than molybdenum memory from a previous experiment. A silver isotope, ^{107}Ag, is seen as an impurity in the lead solution. Comparing the signal of the doubly charged lead ions to that of $^{93}Nb^{+}$, a BEC value of about 0.1 ug L^{-1} is obtained.

Creating greater levels of doubly charged ions is certainly a disadvantage. For most elements the IE' is well above 15 eV.[26] Fortunately, the number of elements affected by interfering M^{2+} ions are few.[27] In some instances the presence of doubly charged metal ions has actually been used to advantage, e.g., for the determination of Eu.[28-30]

Matrix Effects. Space charge repulsion in an ion beam is used as an explanation for the matrix effects in ICP-MS.[31,32] Previous experiments with the graphite injector show that the entire normal analytical zone apparently flows through the orifice of the sampling cone. If the matrix ion density is high in the region of the plasma where sampling occurs, matrix effects might be worse than usual with the graphite injector.

Figure 5 is a graph of the normalized signal for $^{59}Co^{+}$ versus aerosol gas flow rate. The concentration of the concomitant element was held constant at 10 mM. Enhancements are generally not the rule but do occur.[33] The curves for lithium and strontium elevate the Co^{+} signal by about fifty percent.

Sodium concomitant has an interesting effect on cobalt signal. The aerosol gas flow rate that maximizes the $^{59}Co^{+}$ signal shifts to a lower value than in the case where no matrix is present. If this is truly a consistent occurrence then the matrix effect could be eliminated by simply picking operating conditions that produce a "cross-over" point for the two curves. This "cross-over" effect is utilized in ICP-AES[34] but not usually seen in ICP-MS. More work will have to be done to understand this result. As usual, heavy matrix elements like Ba and Pb suppress the Co^{+} signal extensively.

Several tactics for dealing with matrix effects are available. Internal standards can be used with some success. Intrinsic internal standards can result from using polyatomic ions in a spectrum to monitor the effect of a concomitant on an analyte.[35,36] A more stable and reliable internal standard is extrinsically added and can be selected to behave more closely to the analyte of interest.[37] Denoyer et. al. have developed a single focusing lens such that the optimizing potential behaves linearly with respect to elemental mass.[38] The potential on the lens can be optimized to transmit light analyte ions and discriminate against heavy matrix ions. This reduces matrix effects caused by space charge repulsion that occurs inside and after the focusing lens.

This matrix problem can also be minimized by applying a potential to the interface a few volts positive relative to

ground. The idea was applied to a quadrupole instrument with a positive potential applied to the skimmer cone, which produced a greater linear dynamic range for cobalt[39]. Another approach taken to minimize matrix effects is to adjust ion lens potentials to maximize ion transmission for a particular analyte with the matrix present. This was carried out previously with this same instrument and an ion lens configuration like that used in the present work.[19] Figure 6 is a graph of a similar experiment using the graphite injector. The tremendous suppression for Pb matrix seen in figure 5 can be overcome by tuning the voltages applied to lens elements with the Pb matrix present. This result implies that a single internal standard can be selected regardless of what matrix elements are present. Lens potentials used for optimizing with and without the matrix present are shown in Table 4. Though reference 19 did not report similar signal enhancements a similar result was achieved. The 50% improvement in signal for cobalt under the new lens settings without any matrix suggests that these new potentials are a better choice. The ion kinetic energy was about 4 times higher under these conditions which degraded resolution and produced split peaks. More work must be done to understand the results of this experiment.

Conclusions

This paper shows that the level of most polyatomic ions with a graphite injector in an ICP mass spectrum are generally no worse than when using a quartz injector. For some polyatomic ions the BEC values are actually considerably lower. In a least one case, $^{40}Ar^{12}C^{+}$, the polyatomic ion level is much worse and causes a problem for determination of chromium. Doubly charged ions are worse for elements with low second ionization energies. Finally, matrix effects observed with this device are similar to what has been seen previously for ICP-MS. It is possible to adjust lens potentials to mitigate this problem.

Acknowledgements

The authors greatly acknowledge Advanced Ceramics Corp. for donation of the pyrolytic graphite used in this work. Ames Laboratory is operated by Iowa State University for the U.S. Department of Energy under Contract No. W-7405-Eng-82. This research was supported by the Office of Basic Energy Sciences, Division of Chemical Sciences.

References

1. Clemons, P.S.; Minnich, M.;Houk, R.S. *Anal. Chem.* 1995, 67, 1929.
2. Vaughan, M.A.; Horlick, G. *Appl. Spectrosc.* 1986, 4, 434.

3. Tan, S.H.; Horlick, G. *Applied Spectroscopy* 1986, 4, 445.

4. Alves, L.C. Cryogenic Desolvation for Sample Introduction into Inductively Coupled Plasma Mass Spectrometry, Ph.D thesis, Iowa State University, Ames, IA, 1993, Appendix I.

5. Reed, N.M.; Cairns, R.O.; Takaku, Y; Hutton, R.C. *J. Anal. At. Spec.* 1994, 9, 881.

6. Alves, L.C.; Wiederin, D.R.; Houk, R.S. *Anal. Chem.* 1992, 64, 1164.

7. Denoyer, E.R.; Fredeen, K.J.; Hager, J.W. *Anal. Chem.* 1991, 63, 445A.

8. Park, C.J.; Van Loon, J.C.; Arrowsmith, P.; French, J.B. *Can. J. Spectrosc.* 1987, 32, 29.

9. Karanassios, V.; Horlick, G. *Spectochim. Acta*, Part B, 1989, 44B, 1345.

10. Denoyer, E.R. *Atomic Spectroscopy* 1994, 15, 7.

11. Lam, J.W.H.; Horlick, G. *Spectrochim. Acta*, Part B, 1990, 45B, 1313, 1327.

12. Lam, J.W.H.; McLaren, J.W. *J. Anal. At. Spectrom.*, 1990, 5, 419.

13. McLaren, J.W.; Lam, J.W.; Gustavsson, A. *Spectrochim. Acta*, Part B, 1990, 45B, 1091.

14. Smith, F.G.; Wiederin, D.R.; Houk, R. S. *Anal. Chem.*, 1991, 63, 1458.

15. Evans, H.H.; Ebdon, L *J. Anal. At. Spectrom.*, 1990, 5, 425.

16. Nonose, N.; Matsuda, N.; Fudagawa, N.; Kubota,M. *Spectrochim. Acta*, Part B, 1994, 49B, 955.

17. Tanner, S.D. paper presented at the 1995 European Winter Conference on Plasma Spectrochemistry, Jan 8-13, Cambridge, UK., M2.

18. Hu, K.; Clemons, P.S.; Houk, R.S. *J. Amer. Soc. Mass Spectrom.* 1993, 4, 16.

19. Hu, K.; Houk, R.S. *J. Amer. Soc. Mass Spectrom.*, 1993, 4, 28.

20. Ingle, J.D.; Crouch, S.R. *Spectrochemical Analysis*, Prentice Hall, Ch. 8.

21. Larsen, E.H.; Stűrup, S. *J. Anal. At. Spectrom.*, 1994, 9, 1099.

22. Hassegawa, T.; Umemoto, M.; Haraguchi, H.; Hsiech, C.; Montaser, A., in *ICPs in Analytical Atomic Spectrometry*, 2nd ed., Montaser, A; Golightly, D. W., Eds., VCH: New York, 1992, Chap. 8.

23. Hanselman, D.S.; Sesi, N.N.; Huang, M.; Hieftje, G.M. *Spectrochim. Acta*, Part B, 1994, 49B, 495.

24. Furuta, N.; Horlick, G. *Spectrochim. Acta*, Part B, 1982, 37B, 53.

25. Houk, R.S.; Olivares, J.A. *Spectrochim. Acta*, Part B, 1984, 39B, 575.

26. *CRC Handbook of Chemistry and Physics*, Robert C. Weast, ed., 51st Ed., CRC Press, Boca Raton, Florida, 1970.

27. Jarvis, K.E.; Gray, A.L.; Houk, R.S.; *Handbook of ICP-MS*, Blackie, London, 1992, Chap. 5.

28. Date, A.R.; Hutchison, D. *J. Anal. At. Spectrom.* 1987, 2, 269.

29. Jarvis, K.E.; Gray, A.L.; McCurdy, E. *J. Anal. At. Spectrom.*, 1989, 4, 743.

30. Meddings, B.; Ng, R. *Applications of Inductively Coupled Plasma Spectrometry*, eds Date, A.R.; Gray, A.L., Blackie, Glasgow, pp 220-241.

31. Gillson, G.R.; Douglas, D.J.; Fulford, Halligan, K.W.; Tanner, S.D. *Anal. Chem.* 1988, 60, 1472.

32. Tanner, S.D. *Spectrochim. Acta*, Part B, 1992, 47B, 809.

33. Beauchimin, D.; McLaren, J.W.; Berman, S.S. *Spectrochim. Acta*, 42B, 467.

34. Blades, M.W.; Horlick, G. *Spectrochim. Acta*, Part B, 1981, 36B, 881.

35. Beauchimin, D.; McLaren, J.W.; Berman, S.S. *J. Anal. At. Spectrom.*, 1988, 3, 775.

36. Chen, X.; Houk, R.S. *J. Anal. Atom. Spectrom.* 1995, 10, 837.

37. Thompson, J.J.; Houk, R.S. *Appl. Spectrosc.*, 1987, 1, 801.

38. Denoyer, E.R.; Jacqes, D.; Debrah, E.; Tanner, S.D. *Atomic Spectroscopy* 1995, 16, 1.

39. Hu, K.; Houk, R.S.; *J. Am. Soc. Mass Spectrom.*, 1993, 4, 733.

Table 1. Background equivalent concentrations for five common polyatomic ions and sensitivities of corresponding elemental isotopes.

	BEC Values (ppb)					Signal (cts $s^{-1}ppm^{-1}$) X 10^5				
	$^{35}Cl^{16}O$	$^{40}Ar^{12}C$	$^{40}Ar^{14}N$	$^{40}Ar^{16}O$	$^{40}Ar^{35}Cl$	^{51}V	^{52}Cr	^{54}Fe	^{56}Fe	^{75}As
Graphite Injector	3.1	12	4.2	2.4	0.34	16	15	2.4	37	8.7
Quartz Injector	21	1.4	9.2	1.2	6.0	11	10	0.93	15	2.5

Table 2. Signal levels for singly and doubly charged analyte ions. Analytes prepared at a concentration of 0.1 ppm in 1% HNO_3.

		Injector Type			
		PIGI (cts/s)		Quartz (cts/s)	
Element	2nd I.E. (eV)	M^+ ($x10^5$)	M^{+2}	M^+ ($x10^5$)	M^{+2}
^{138}Ba	10.004	3.4	10800	2.2	1180
^{141}Pr	10.55	5.0	5170	3.3	1060
^{139}La	11.06	3.2	4120	2.6	960
^{169}Tm	12.05	4.2	1970	1.4	410
^{93}Nb	14.32	4.9	650	2.45	170
^{208}Pb	15.032	1.7	70	1.0	60

Table 3. Relative values of doubly charged analyte ions. Analyte and internal standards present at 0.1 ppm.

		Injector Type	
Ratio	2nd I.E.(eV)	PIGI	Quartz
M^{+2}/M^{+}			
Ba^{+2}/Ba^{+}	10.004	0.0313	0.00538
Pr^{+2}/Pr^{+}	10.55	0.0103	0.00322
La^{+2}/La^{+}	11.06	0.0128	0.00364
Tm^{+2}/Tm^{+}	12.05	0.00467	0.00300
Nb^{+2}/Nb^{+}	14.32	0.00133	0.000711
Pb^{+2}/Pb^{+}	15.032	0.000413	0.000595
$M^{+2}/(int.std)^{+}$			
Ba^{+2}/Co^{+}	10.004	0.0643	0.0123
Pr^{+2}/Co^{+}	10.55	0.0310	0.0105
La^{+2}/Co^{+}	11.06	0.0304	0.0108
Tm^{+2}/Co^{+}	12.05	0.0127	0.00422
Nb^{+2}/Co^{+}	14.32	0.00520	0.00221
Pb^{+2}/Ag^{+}	15.032	0.000642	0.000910

Table 4. Optimized potentials for maximum $^{59}Co^{+}$ signal with no matrix and a 10 mM Pb matrix. For identification of lens elements see ref. 19.

Lens Voltages (volts)

Lens No.	No Matrix	10 mM Pb Matrix
1	+ 6	+ 11
2	- 100	- 425
3	- 250	+ 10
4	+ 6	+ 10
5	- 500	- 500
6	+ 6	+ 10
7	-75	- 75

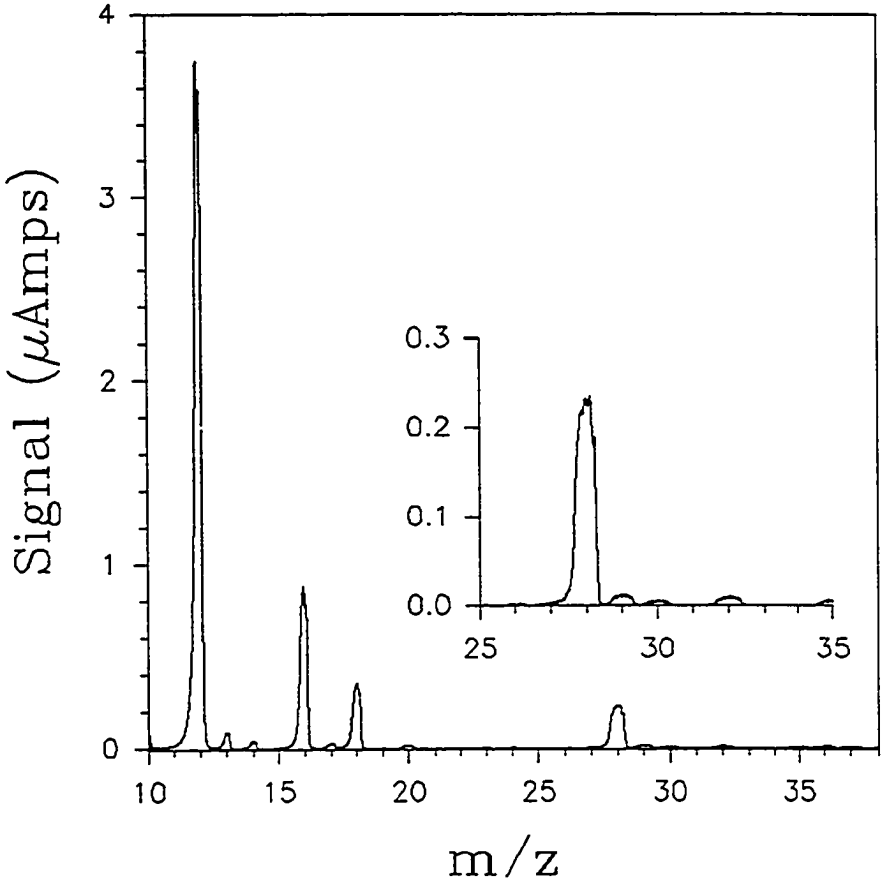

Figure 1. Low mass spectrum obtained with a graphite injector and alumina support tube while nebulizing deionized water. The inset spectrum shows a prominent peak at m/z= 28. The O_2^+ signal is attenuated compare to a conventional quartz torch.

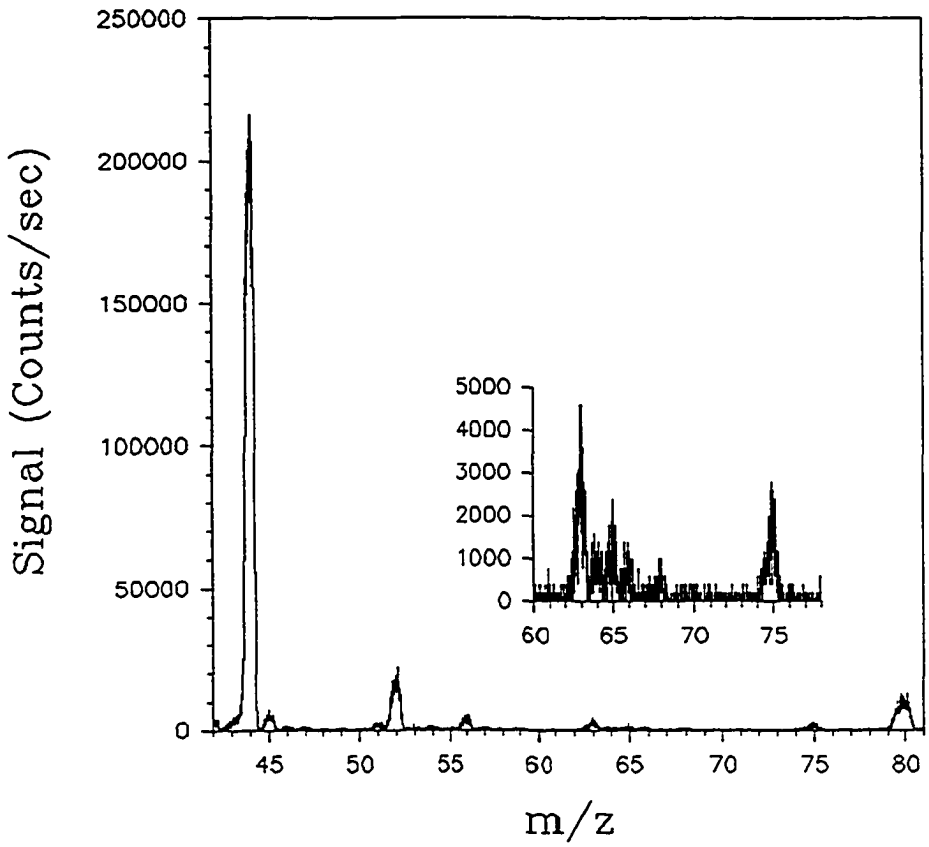

Figure 2. Mid-mass spectrum of background ions using a graphite injector and an alumina support tube while nebulizing deionized water. Inset spectrum shows background copper ions at m/z= 63 and 65. Also, some As memory is present at m/z= 75.

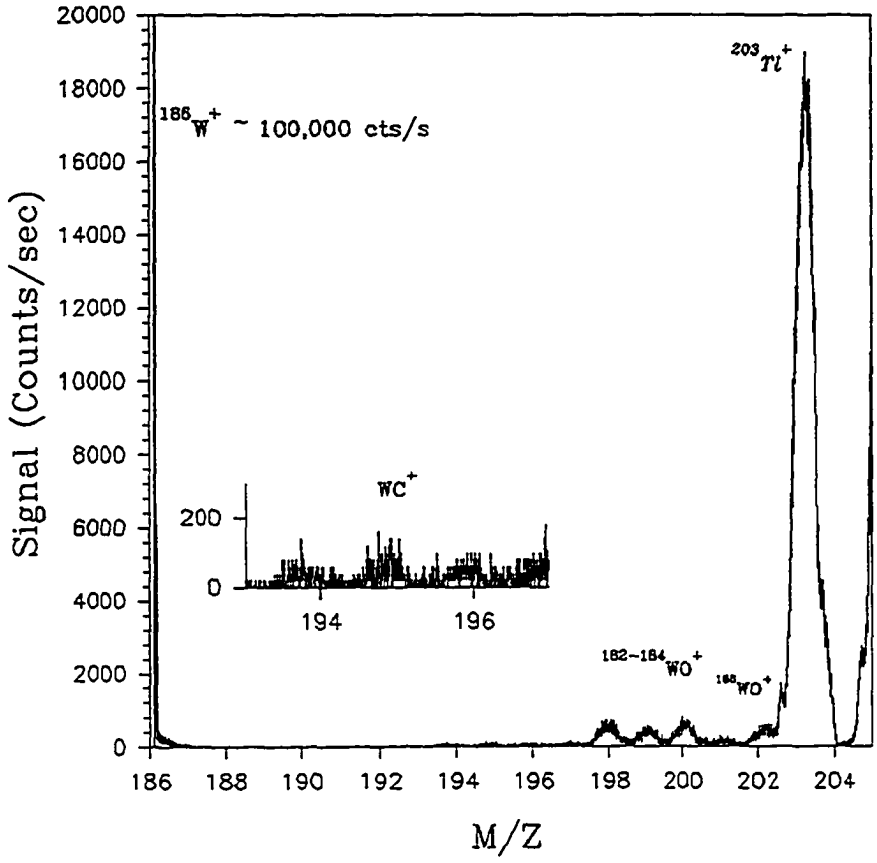

Figure 3. A spectrum of oxides and carbides of tungsten from a graphite injector. Tungsten solution concentration is 50 mg L^{-1} and thallium is at 50 ug L^{-1} as an internal standard. Inset spectrum shows peaks of WC^{+}.

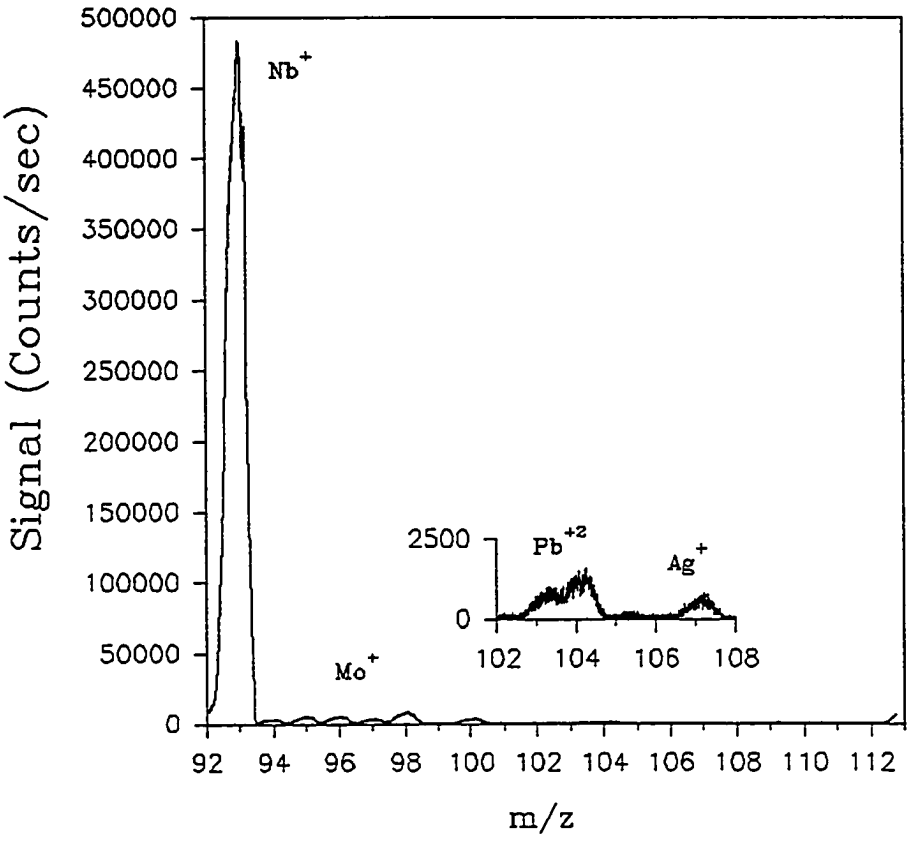

Figure 4. Spectrum of doubly charged lead ions taken with a graphite injector. Lead solution concentration is 1 mg L^{-1}. Isotopes of molybdenum are from memory in the spray chamber. Inset spectrum shows unresolved doubly charged lead isotopes and some silver impurity.

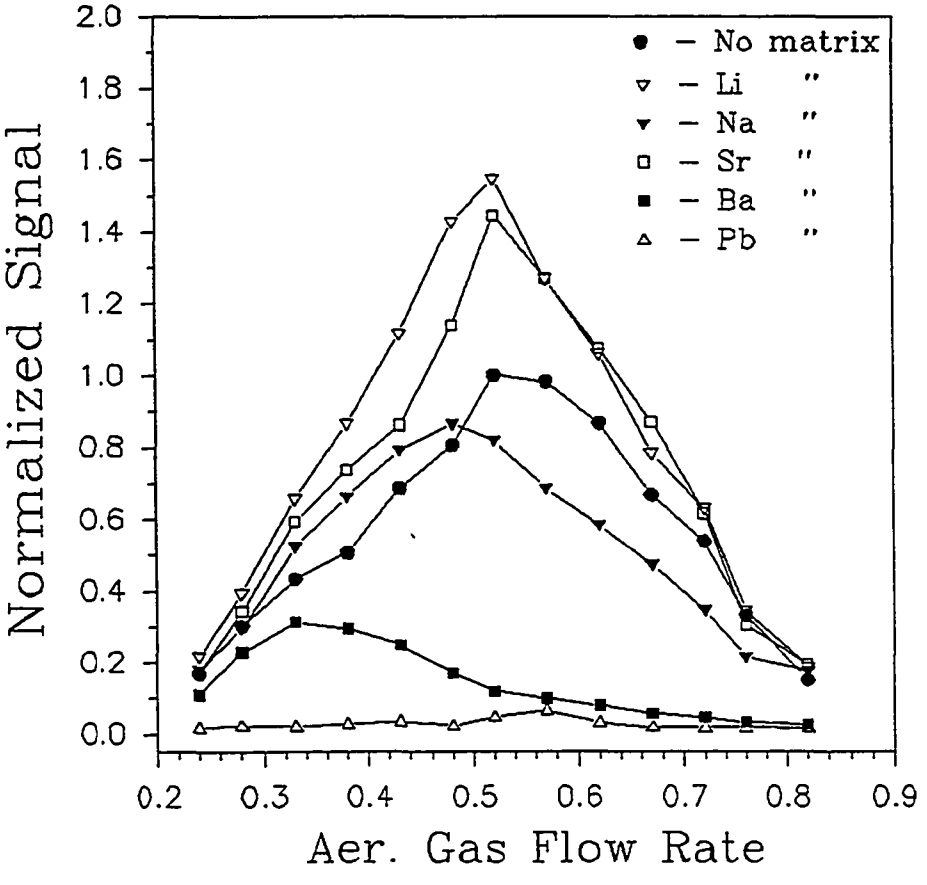

Figure 5. Matrix effects as a function of aerosol gas flow rate while using a graphite injector. Cobalt is present at 0.5 mg L^{-1} in a varying elemental matrix at 10 mM.

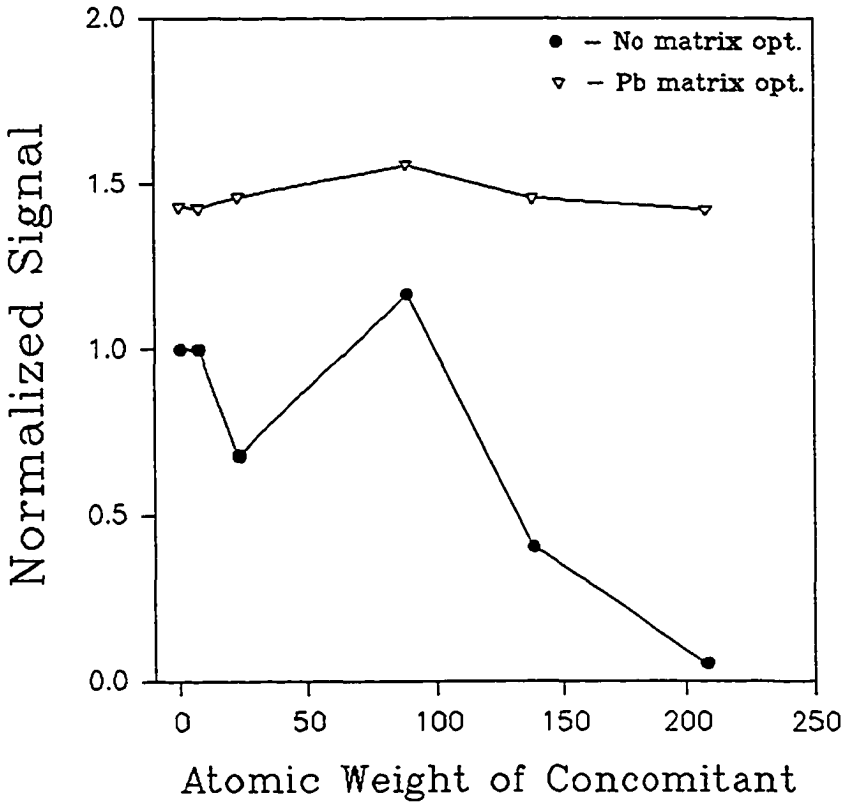

Figure 6. Matrix effect as a function of concomitant mass. Each of the 6 solutions contains Co at o.5 mg L^{-1}. For the left most points, the solution contained only Co. For the other points, either Li, Na Sr, Ba or Pb was present at 10 mM. Optimization of lens elements with lead matrix present results in elimination of matrix effects and provides a 50% improvement in Co^{+} signal over lens settings optimized with no matrix present.

CHAPTER 4. THE ROLE OF CARBON DURING THE USE OF A GRAPHITE INJECTOR FOR INDUCTIVELY COUPLED PLASMA MASS SPECTROMETRY

P. Scott Clemons, Narong Praphairaksit and R. S. Houk[1]

A paper submitted for publication to Spectrochimica Acta, Part B, Atomic Spectroscopy

Abstract

The role of carbon during the use of a graphite injector (GI) for inductively couple plasma mass spectrometry (ICP-MS) is investigated. Graphite tubes are made from spectroscopic (SG) and pyrolytic graphite (PG) and inserted into an alumina support tube to create an injector device that replaces the normal quartz injector of a demountable torch. SG erodes at five times the rate of PG, thus putting more carbon into the plasma. The MO^+ signal is dependent on the amount of carbon in the plasma. This result is correlated to an atomization mechanism in a graphite furnace where carbon reduces metal oxides to produce free metal atoms and carbon monoxide. Also, the extra enhancement of As^+ and Se^+ signals is attributed to a

---

[1]Corresponding author

charge transfer reaction between C^+ and the respective neutral atom. The amount of enhancement is dependant on the density of C^+ in the plasma.

Introduction

Graphite furnace atomic absorption (GFAA) is one of the most sensitive analytical techniques for the determination of a large number of metallic elements.[1,2] Such a furnace is generally an efficient atomization source. Several recent fundamental investigations of the graphite furnace have centered around analyte atomization mechanisms. Thermodynamic considerations suggest that direct oxide dissociation and carbon reduction of oxides are possible.[3,4] Atomic spectrometry has been used to understand the radial dependence of atomization within the atomization tube.[5-7] Mass spectrometry can monitor furnace species directly as shown in several publications.[8-15] Several of these investigations show that carbon plays a major role in atomization for many elements. In particular, carbon produces a reducing atmosphere, which helps remove metal oxides.[16]

A graphite furnace can also be used to inject sample into an inductively coupled plasma mass spectrometer (ICP-MS).[17-19] Unfortunately, a GF yields transient signals. This is often a problem for small samples regarding sensitivity and signal integration requirements. Precision is generally poor with a

relative standard deviation as high as 20%.[20] The time limitations of peak hopping contribute to poor precision and reduce the multielement capabilities of an ICP-MS unless the instrument has multichannel detector capabilites.[21,22]

ICP-MS has a problem with spectral interference caused by metal oxide ions. Much work has focused on removing or at least attenuating these troublesome ions[23-26]. It would be an advantage to use the atom production mechanism of a GF with continuous sample introduction. This combination could greatly reduce the metal oxide ion levels observed in the mass spectrum.

Recently, an injector device using a graphite tube for an ICP torch has been described for ICP-MS.[27] This paper connects what is known about atom production in a GF to some of the results obtained with the graphite injector. For example the density of graphite in the plasma is related to the low metal oxide signals obtained with this device.

Many fundamental investigations of the ICP have focused on ionization and excitation mechanisms. Of these, charge transfer reactions (CT) have been shown to play a minor yet definite role in analyte ion production for certain elements. Most work has investigated the transfer of charge from argon ions to neutral analyte atoms.[28-34] More recently, a CT reaction involving xenon ions and neutral iron atoms has been described.[35] In the present work the density of carbon atoms

and ions in the ICP can be controlled by choosing the type of carbon used for the injector tip. The extensive signal enhancements observed for As^+ and Se^+ indicate that these ions are formed partly by CT reactions between carbon ions and these analyte atoms.

Experimental

The ICP-MS device was made in house and has been described before.[36] The skimmer orifice has become slightly larger than that of the sampling cone. This situation reportedly increases the level of metal oxide ions.[37,38] General operating conditions used with the graphite injector have been described.[27] Sample aerosol was produced by an ultrasonic nebulizer with desolvation. Cryogenic desolvation was not applied in these experiments. Operating conditions (forward power, nebulizer gas flow, sampling position and ion lens voltages) were selected to maximize the analyte signal for each injector used.

Injector Tip Material. Two types of graphite were used for this work. Pyrolytic graphite (PG) was donated by Advanced Ceramics Corp. (Cleveland, OH) and machined to be press fit into an alumina support tube.[39] A similar tube of spectroscopic graphite (SG) was machined from a DC arc electrode (Bay City Carbon, Bay City, MI). Injector tips were 2 mm i.d. x 5 mm o.d. and about 2.5 cm long, as before.[27]

Both types of graphite were leached in acid (usually 5% HCl) overnight prior to use. Background scans were performed before each experiment to ensure analyte ion signals were not compromised by contaminants in the graphite. Both the graphite injectors and a conventional quartz injector were operated with the same demountable torch.

Data Acquisition. The output of the Channeltron electron multiplier was connected to either a current-to-frequency converter or pulse counting equipment.[39] Background spectra were signal averaged by sweeping the mass range of m/z= 10 to 45 All other data were collected over window 20 mass units wide. Lanthanum and lanthanum oxide signals were integrated over 100 sweeps; other signals were integrated over 50 sweeps. The multichannel analyzer divided the observed mass window equally into 4096 channels. Also, the quadrupole was set to achieve unit mass resolution or better.

Solutions. All analyte solutions were made with standard stock solutions (1000 mg L^{-1}, Plasma Chem) and diluted to the appropriate volume with 1% aqueous HCl. Lanthanum for metal oxide measurements was made at a concentration of 0.1 mg L^{-1}. All other analytes were present at 7.17 μM. Deionized water was obtained from an in house system (Barnstead, 18 MΩ).

Results and Discussion

Erosion Rate. The most common type of atomization furnace uses a graphite tube made from pyrolytic graphite (PG) and randomly ordered graphite, which we call spectroscopic graphite (SG). SG is more porous than PG and has a lower sublimation temperature, about 3300 °C.[40] PG is much less porous and also more temperature resistant with a reported melting point of about 4300 °C.[41] Thus, PG is usually preferred as a graphite furnace for its lifetime and reduced memory effects.

Comparing the two materials as tips for our graphite injector, PG would obviously be the most robust in an ICP. Two tips were constructed from PG and SG and then operated for about one hour in the plasma under typical operating conditions for this device. The mass of the tip was measured before and after, and the average erosion rate was determined from the mass loss. SG eroded at an average rate of about 11 $\mu g\ s^{-1}$ compared to 2.2 $\mu g\ s^{-1}$ for PG. This implies that there is almost five times more carbon being introduced into the plasma when using SG compared to PG. If carbon does play a role in producing low metal oxides and increasing sensitivity of some elements, as previously seen, then experimental comparison of these two materials with a normal quartz injector (QI) should help answer this question.

Background Ions. Figures 1 thru 3 are spectra of background ions produced under usual analytical conditions while using a QI, PG and SG tip injectors respectively while nebulizing deionized water. The spectrum in Figure 1A shows the major background ions. Oxygen ($^{16}O^+$) and water ($H_2{}^{16}O^+$) are the dominant ions in the lower mass range. These peaks are present in about the same abundance and are expected even when the bulk of the water is removed by desolvation. The next substantial peak is $^{16}O_2{}^+$. Finally, $^{40}Ar^+$ and $^{40}ArH^+$ appear at the typical abundance for these ions in an argon ICP.

Comparison of these spectra to that of Figure 2A reveals some interesting changes. A substantial peak for $^{12}C^+$ is observed using the PG injector. The $^{16}O^+$ and $H_2{}^{16}O^+$ peaks are about the same intensity as those found with the QI. A new peak is present at m/z= 28. Given that the signal for $^{14}N^+$ has not increased substantially this intensity cannot be attributed to the $^{14}N_2{}^+$. The next obvious choice would be carbon monoxide ions, $^{12}C^{16}O^+$. The $^{12}C^+$ and $^{12}C^{16}O^+$ signals are of similar abundance. Next, notice that the $^{16}O_2{}^+$ signal has been slightly attenuated compared to Figure 1.

The spectrum shown in Figure 3 was obtained with a SG tip. Carbon is now much more abundant than the $^{16}O^+$ and $H_2{}^{16}O^+$ peaks. The signal for $^{16}O^+$ is about the same but the number of water ions seem to be reduced by half compared to the two previous spectra. The signal for $^{12}C^{16}O^+$ has also increased and

the ratio of $^{12}C^{+}$ to $^{12}C^{16}O^{+}$ is now about ten to one. Both the PG and SG injector also produce a noticeable signal from $^{12}C^{16}O_2^{+}$.

Relation to Atomization Mechanisms in GF. The results of Figures 1 through 3 show that the carbon from the graphite tips can produce $^{12}C^{16}O^{+}$ and attenuate O_2^{+}. The difference in the relative intensities of Figures 2 and 3 can be related to atomization phenomena in a GF. The reaction:

$$C(s) + 1/2O_2(g) \rightarrow CO(g) \qquad (1)$$

becomes thermodynamically favorable at higher temperatures[42,43]. The change in the Gibbs free energy at 1000 °C is about -48 kcal/mol.[44] Carbon can also reduce O_2 to produce CO_2 and react with H_2O to form CO and H_2 gas. These latter reactions are also more favorable at elevated temperatures. Typical temperatures inside a GF reach about 2000 to 2500 °C. Given that our graphite tip glows a bright orange, we estimate the temperature to be about 2000 °C based upon temperature plots for black body radiance.[45] A calculated plot of carbon flux versus temperature has been prepared by Gilmutdinov et. al.[42] From our carbon loss experiment the corresponding carbon flux gives a temperature of about 2400 °C for SG and 2100 °C for PG. Reaction 1 is a surface reaction and it has been attributed to certain active sites on the graphite surface.[44] The inner surface of SG "erodes" faster than that of PG, so it

makes sense that SG would have more active sites available for reaction 1 than PG.

Sturgeon et. al. suggest four general atomization mechanisms in a GF.[4] The reduction of metal oxides by carbon is among these and can be written as follows:

$$2MO(s) + 2C(s) \rightarrow 2CO(g) + 2M(s) \rightarrow M_2(g) \rightarrow 2M(g) \quad (2)$$

Equation 2 represents solid phase metal oxide being reduced by solid phase carbon to produce free gaseous metal atoms. Carbon reduction of metal oxides also occurs on the graphite surface, as with reaction 1. Carbon vapor can also condense on the cooler surface of oxide microparticles followed by diffusion into the analyte oxide particle.[46] It is thought that the reduction reaction is delayed until a certain stoichiometry of the reactants has been achieved, yet this is not certain.

Also, as with reaction 1, reduction of metal oxides by carbon is thermodynamically favorable at higher temperatures.[3] A mathematical model of the temperature inside the graphite tip shows that the argon gas from the nebulizer quickly reaches the temperature of the surrounding graphite wall.[47] This work also suggests turbulence exists at the upstream end of the injector tip. This is a result of the cool argon gas from the desolvation system entering the hot environment inside the graphite tip. This could be an advantage as

analyte particles in the bulk portion of the entering gas would have a greater chance of being swept to the hot graphite surface. Once CO is formed the molecule must withstand the temperatures of the plasma. The free oxygen could form MO^+ with metal ions in the boundary layer of the interface.[37,38] The authors of ref. 42 suggest that CO dissociation in the plasma is negligible.

Metal Oxide Levels. Table 1 compares La^+ and LaO^+ signals when using the three injectors of Figures 1 through 3. Both relative and absolute levels of MO^+ ions are reduced when using a graphite injector of either type. SG attenuates the MO^+ by a factor of two more than PG. Compared to the QI, SG shows a LaO^+/La^+ that is seven times lower. The absolute metal oxide ion signal for SG is about three times lower than that for the QI. These improvements in MO^+/M^+ are not as substantial as those in ref. 27. The enlarged skimmer orifice is a suspected problem.

Carbon Density and Enhanced Analyte Ionization. The general problem of poor sensitivity for elements of high ionization energy (IE) plagues their determination by ICP-MS. In a previous report we commented on the ability of the graphite injector to increase the sensitivity of a wide range of elements.[27] The general result is that the signal for elements of high IE experience a greater enhancement over the QI injector signals for easily ionized elements. This

enhancement was partly attributed to the narrowing of the normal analytical zone (NAZ). The sampling orifice collects a greater fraction of the ions in this region of the plasma. Also, the ions can be sampled from a region of the NAZ where the "temperature" for the analytes is highest when the graphite injector is used. If so, the higher the IE, the greater the signal enhancement.

During our comparison of PG and SG an interesting result was observed. Table 2 gives relative ion signals for As^+, Se^+, Zn^+ and Br^+ which are compared to the ion signal for $^{69}Ga^+$. Each element is present in equimolar concentrations. They are chosen such that their small mass difference would not produce large mass bias effects. Table 3 shows the absolute signal for these four elements. The relative signals of $^{75}As^+$ (with the contribution of $^{40}Ar^{35}Cl^+$ removed), and $^{78}Se^+$ show substantial improvements when using a GI compared to a QI. Also, there is a significant improvement when using a SG tip over a PG tip for these elements. The signal for $^{64}Zn^+$ also improves with a GI over a conventional QI, but there is little difference between the SG and PG injector tips. The relative signal for bromine (Br^+/Ga^+) is unchanged with any of the injectors used. Table 3 shows the same general trends for the absolute signals; i.e., both SG and PG yield the same signal improvements compared to the conventional injector .

These results can be explained as follows. Signals for

all elements are enhanced when using a GI compared to a QI. This is due to the constriction of the NAZ, as discussed before. For some elements (e.g., Zn), the enhancement when using PG is similar to that from SG, these elements probably experience a thermal environment that favors ionization. Bromine behaves like zinc with respect to SG and PG injector tips but does not show the same magnitude of enhancement as zinc compared to a QI. The large enhancements observed with As and Se are probably related to the density of carbon in the plasma. Others have noticed large signal enhancements for As by adding carbon as an organic solvent in the analyte solution[48]. This result could be due to the presence of carbon in the plasma. It is also possible that the smaller droplet size distribution of the organic-water solution favors more efficient vaporization and atomization within the plasma.[49] Introducing carbon directly into the plasma by inserting a graphite tip does not effect nebulization. We believe this result is due to charge transfer (CT) reactions between carbon ions and As and Se atoms in the plasma. CT reactions between analyte atoms and argon ions,[29-35] and more recently Xe ions,[36] have been investigated by others as an ionization mechanism in the ICP.

If carbon ions are to be involved in a CT reaction their density must be sufficiently high in the plasma. From the earlier discussion on carbon loss from SG, about 5.5×10^{17} atoms

s^{-1} enter the central channel of the plasma. At an aerosol gas flow rate of 0.5 L min^{-1} and a gas temperature of 5000 K there should be a carbon atom density of $4x10^{15}$ atoms cm^{-3}. This should give a carbon ion density (n_{C^+}) of about $2x10^{14}$ ions cm^{-3}, if carbon is about 5% ionized in an ICP.[50] Using the same argument for PG, n_{C^+} is about $4x10^{13}$ ions cm^{-3}. If the cross section for the reaction is similar to that for the Xe^+ and Fe system of ref. 35 then there should be a sufficient density of carbon ions. In addition, using SG should drive the CT reaction more extensively than PG.

For an efficient CT reaction, the energy difference between the electronic states of the carbon ion and analyte ions should be small. An acceptable energy defect is up to ~0.5 eV, the average thermal collision energy in the ICP at 5000 K. Figures 4 and 5 give partial energy diagrams for C, As, Se, Zn and Br.[51] Only the energy level of the ground state of the carbon ion is shown. The energy level of the first excited state of C^+ is 16.59 eV above C^+ ($^2P_{1/2}$).

The first excited state for the arsenic ion, $As^+(^1D_2)$, at 11.06 eV, is only 0.20 eV below that of $C^+(^2P_{1/2})$, 11.26 eV. The following reaction is possible:

$$C^+(^2P_{1/2,3/2}) + As(^4S_{3/2}) \rightarrow C(^2P_{0,1,2}) + (As^+)(^1D_2) \qquad (3)$$

In general, CT reactions are allowed if they involve a) a small energy defect and b) changes in configuration only of

the outer electrons, not core electrons.[35] This reaction transfers an outer shell p electron from arsenic to a carbon ion such that $As(4s^24p^3)$ goes to $As^+(4s^24p^2)$ and $C^+(2s^22p^1)$ goes to $C(2s^22p^2)$. The energy difference between the excited state arsenic ion and the ground state carbon ion is small enough for a CT reaction.

The first excited state of the selenium ion, $Se^+(^2D_{1/2})$, at 11.36 eV is only 0.12 eV above $C^+(^2P_{1/2})$, giving the following reaction:

$$C^+(^2P_{1/2,3/2}) + Se(^3P_{2,1,0}) \rightarrow C(^2P_{0,1,2}) + (Se^+)(^2D_{3/2,5/2}) \quad (4)$$

Again, this reaction involves the transfer of an outer shell p electron; $Se(4s^24p^4)$ goes to $Se^+(4s^24p^3)$ and $C^+(2s^22p^1)$ goes to $C(2p^2)$. This reaction also involves only a small energy difference between the states of Se^+ and C^+. The additional energy (0.12 eV) necessary to drive the reaction could be provided by the KE of the collision at T~5000 K.

Zinc and bromine show the largest energy differences. The zinc ion, $Zn^+(^2S_{1/2})$, at 9.391 eV is 1.87 eV below the ground state carbon ion, $C^+(^2P_{1/2})$. The next highest level of Zn^+ is $Zn^+(^2P_{1/2})$, which is 4.14 eV above the ground state carbon ion. Neither Zn^+ level is close enough for charge transfer from C^+. The bromine ground state ion, $Br^+(^3P_2)$, at 11.84 eV is 0.58 eV above $C^+(^2P_{1/2})$. This difference seems small enough, yet, the Br^+ levels observed for PG and SG

suggest a CT reaction does not take place. This reaction is probably too endothermic.

Conclusion

This work shows that carbon introduced while using a graphite injector has a significant effect on levels of $^{12}C^{16}O^+$ and $^{16}O_2^+$. The level of metal oxide ions is lower when the carbon density in the plasma is high. We also believe that a charge exchange reaction has been proposed that explains some of the signal enhancements observed in previous work by several groups. The key to this investigation was choosing carbon materials for the injector tip that introduce different levels of carbon into the plasma. Further work should be performed to investigate other analyte ions that might experience signal enhancement through this type of reaction.

Acknowledgements

The authors would like to thank Advanced Ceramics Corp. for donation of the pyrolytic graphite. Ames Laboratory is operated by Iowa State University for the U.S. Department of Energy under contract No. W-7405-Eng-82. This research was supported by the Office of Basic Energy Sciences, Division of Chemical Sciences.

References

1. L'vov, B. V. *Spectochim. Acta*, Part B, 1984, 39B, 159.

2. Slavin, W. *Graphite Furnace AAS: A Source Book*, Perkin-Elmer , Ridgefield, CT 1984, vii.

3. Campbell, W. C.; Ottaway, J. M. *Talanta* 1974, 24, 837.

4. Sturgeon, R. E.; Chakrabarti, C. L. *Prog. Anal. At. Spectosc.* 1978, 1, 5

5. Salmon, S. G.; Holcombe, J. A. *Anal. Chem.* 1979, 51, 648.

6. Holcombe, J. A.; Rayson, G. D., Akerlind, N. *Spectrochim. Acta*, Part B, 1982, 37B, 319.

7. Gilmutdinov, A. Kh.; Zahkarov, Yu. A; Ivanov, V. P.; Voloshin, A. V. *J. Anal. Atom. Spectrom.* 1991, 6, 505.

8. Styris, D. L.; Kaye, J. H. *Spectrochim. Acta*, Part B 1981, 36B, 41.

9. Styris, D. L. *Anal. Chem.* 1984, 56, 1070.

10. Sturgeon, R. E.; Mitchell, D. F.; Berman, S. S. *Anal. Chem.* 1983, 55, 1059.

11. Bass, D. A.; Holcombe, J. A. *Anal Chem* 1987, 59, 974.

12. Ham, N. S.; McAllister, T. *Spectrochim. Acta*, Part B 1988, 43B, 789.

13. Styris, D. L. Fresenius S. *Anal. Chem.* 1986, 323, 710.

14. Byrne, J. P.; Hughes, D. M.; Chakrabarti, C. L.; Gregoire, D. C. *J. Anal. At. Spectrom.* 1994.

15. Park, C. J.; van Loon, J. C.; Arrowsmith, J,; French, J. B. *Can. J. Spectrosc.* 1987, 32, 29.

16. Styris, D. L.; Redfield, D. A. *Spectrochim. Acta Rev.* 1993, 15, 71.

17. Gregoire, D. C.; *J. Anal. Atom. Spectrom.* 1988, 3, 309.

18. Newman, R. A.; Osborn, S; Siddik, Z. H. *Clin. Chim. Acta* 1989, 179, 191.

19. Lamoureaux, M. M.; Gregoire, D. C.; Chadrabarti, C. L.; Goltz, G. M. *Anal. Chem.* 1994, 66, 3217.

20. Jarvis, K. E.; Gray, A. L.; Houk, R. S. *Handbook of ICP-MS*, Blackie, Lodon, 1992, Ch. 4.2.

21. Walder, A. J.; Freedman, P. A. J. Anal. Atom. Spectrom. 1992, 7, 571.

22. Warren, A; Allen, L; Pang, H. M.; Houk, R. S.; Jangorbani M. *Appl. Spectrosc.* 1994, 48, 1360.

23. Alves, L. C.; Weiderin, D. R.; Houk, R. S. *Anal. Chem.* 1992, 64 1164.

24. Denoyer, E. R.; Fredeen, K. J.; Hager, J. W. *Anal. Chem.* 1991, 63, 445A.

25. Shibata, N; Fugadawa, N; Kubota, M. *Spectrochim. Acta*, Part B, 1993, 48B, 1127.

26. Karanassios, V; Horlick, G *Spectrochim. Acta*, Part B, 1989, 44B, 1354.

27. Clemons, P. S.; Minnich, M; Houk, R. S. *Anal. Chem.* 1995, 67, 1929.

28. Batal, A.; Mermet; J. M. *Can. J. Spectrosco.* 1982, 27, 37.

29. Goldwasser, A.; Mermet, J. M. *Spectrochim. Acta*, Part B, 1986, 41B, 75.

30. van der Mullen, J. M.; I. M. Raaijmakers; van Lammeren, A. P; Schramm, D. C.; van der Sijde, B.; Schenkelaars, H. J. *Spectrochim. Acta*, Part B, 1987, 42B, 1039.

31. Burton, L. L.; Blades, M. W. *Spectrochim. Acta*, Part B, 1991, 46B, 819.

32. Farnsworth, P. B.; Smith, B. W.; Omenotto, N. *Spectrochim. Acta*, Part B, 1991, 46B, 843.

33. Ogilvie, C. M.; Farnsworth *Spectrochim. Acta*, Part B, 1992, 47B, 1389.

34. Farnsworth, P. B.; Omenetto, N. *Spectrochim. Acta*, Part B, 1993, 48B, 809.

35. Bricker, T. M.; Smith, F. G.; Houk, R. S. *Spectrochim. Acta*, Part B, 1995, 50B, 1325

36. Hu, K; Clemons, P. S.; Houk, R. S *J. Am. Soc. Mass Spectrom*, 1993, 4, 16.

37. Gray, A. L. *Spectrochim. Acta*, Part B, 1986, 41B, 151.

38. Vaughn, M. A.; Horlick, G. *Spectrochim. Acta*, Part B, 45B, 1289.

39. Clemons, P. S.; Praphairaksit, N.; Houk, R. S. *Spectrochim. Acta*, Part B, submitted.

40. Riley, M. W. *Mater. Design Eng.* 1962.

41. Venkatesan, T.; Jacobson, D. L.; Gibson, J. M. *Phys. Rev. Lett.* 1984, 53, 360.

42. Gilmutdinov, A.; Staroverov, A. E.; Gregoire, D. C.; Sturgeon, R. E.; Chakrabarti, C. L. *Spectrochim. Acta*, Part B, 1994, 49B, 1007.

43. Chakrabarti, C. L.; Chang, S. B.; Roy, S. E. *Spectrochim. Acta*, Part B, 1983, 38B, 447.

44. Kinoshita, K. *Carbon: Electrochemical and Physicochemical Propertieso*, John Wiley and Sons. 1988, Ch. 4.

45. Winfordner, J. D.; Schulman, S. G.; O'Haver, T. C. *Luminescence Spectrometry in Analytical Chemistry*, Wiley-Interscience, New York, 1972.

46. L'vov, B. V.; Savin, A. S. *J. Anal Chem* (USSR), 1982, 37, 2116.

47. Clemons, C. B.; Hariharan, S. I.; Young, G.; Clemons, P. S.; Houk, R. S. to be published.

48. Larsen, E. H.; Stürup, S *J. Anal. At. Spectom.* 1994, 9, 1099.

49. Shum, S. C. K.; Johnson, S. K.; Pang, H. M.; Houk, R. S. *Appl. Spectrosc.* 1993, 47, 575.

50. Houk, R. S. *Anal. Chem.* 1986, 58, 97A.

51. Moore, C. E. *Atomic Energy Levels*, NBS Circular 467, U. S. Government Printing Office, 1949, 1, 211.

Table 1. Effect of carbon on the level of metal oxide observed. A solution of 0.1 mg L^{-1} solution of lanthanum was used as the analyte solution.

	Count Rate (counts s^{-1})		
	$La^+(x10^5)$	LaO^+	LaO^+/La^+
Spectroscopic Graphite	4.54	380	0.00083
Pyrolytic Graphite	2.54	435	0.00172
Normal Quartz Injector	2.12	1265	0.0060

Table 2. Effect of injector type and carbon content on relative analyte signal. Analyte concentration is 7.17 μM.

	Signal Ratio		
Species	Spectroscopic	Pyrolytic	Quartz
$^{75}As^{+}/^{69}Ga^{+}$	0.688	0.390	0.173
$^{78}Se^{+}/^{69}Ga^{+}$	0.164	0.0496	0.0270
$^{64}Zn^{+}/^{69}Ga^{+}$	1.48	1.50	0.460
$^{81}Br^{+}/^{69}Ga^{+}$	0.00403	0.00452	0.00442

Table 3. Effect of injector type and carbon content on absolute analyte signal. Analyte present at 7.17 μM.

	Analyte Count Rate ($x10^4$ counts s^{-1})		
Elements(I.E.,eV)	Spectroscopic	Pyrolytic	Quartz
$^{75}As^+$	19.2	14.4	3.75
$^{78}Se^+$	4.87	1.33	0.500
$^{64}Zn^+$	38.7	43.4	5.12
$^{81}Br^+$	0.119	0.146	0.085

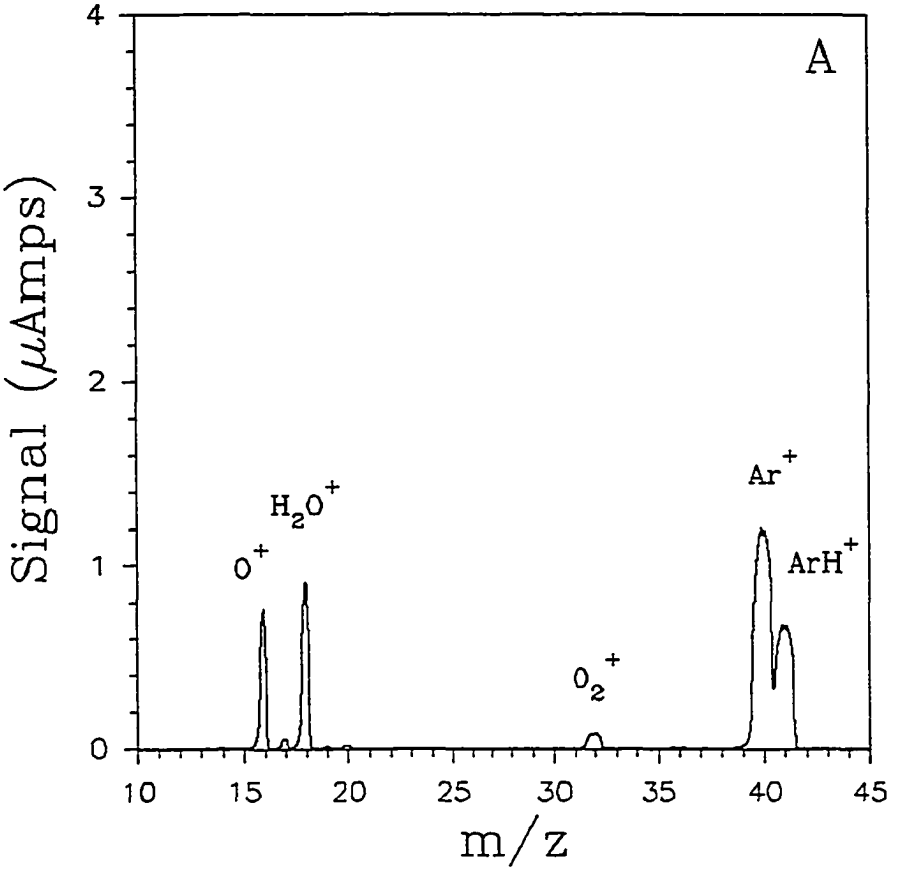

Figure 1. Background spectrum of deionized water taken while using a normal quartz injector (QI).

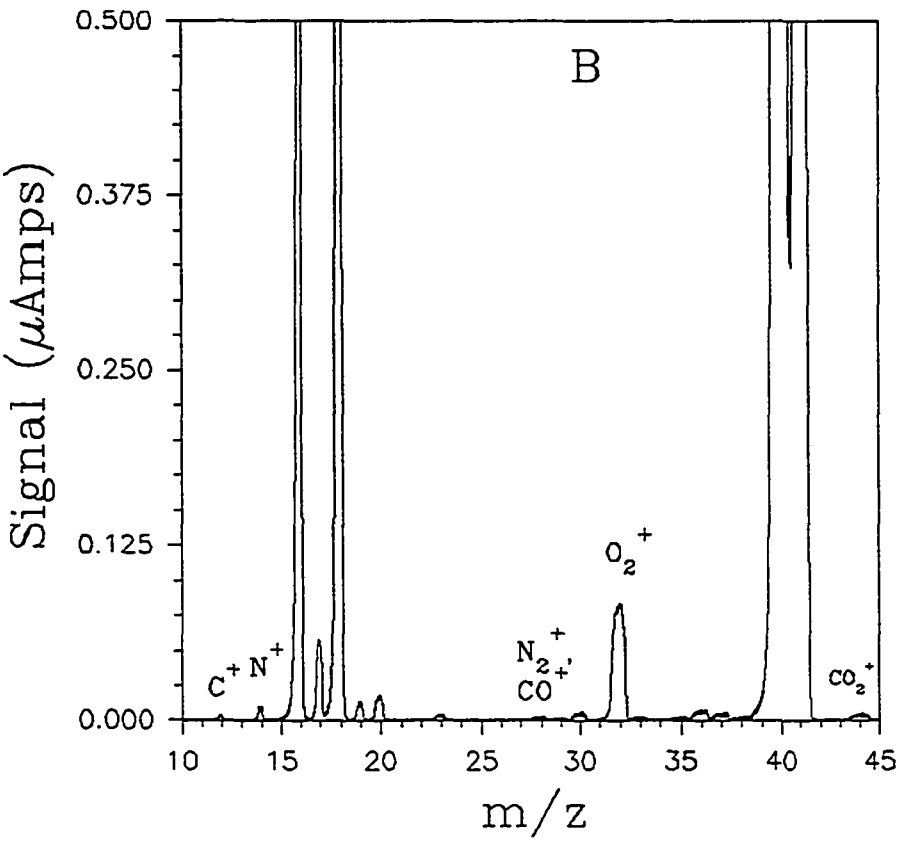

Fig.1 (continued)

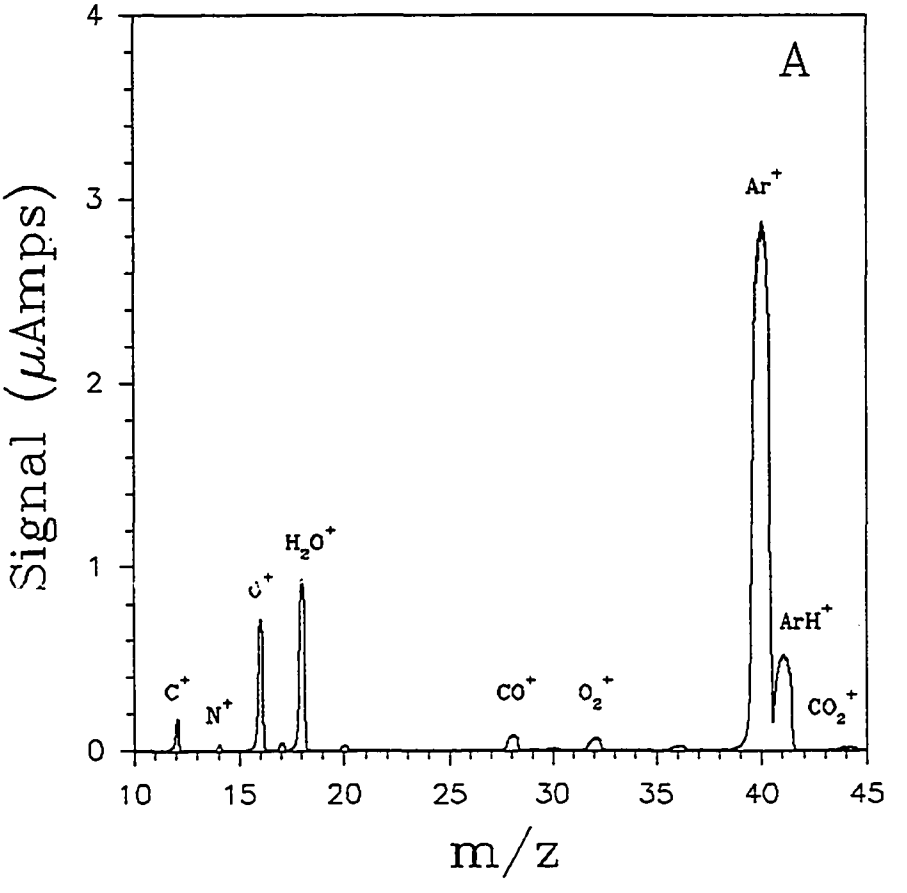

Figure 2. Background spectrum of deionized water taken while using a graphite injector made from pyrolytic graphite (PG).

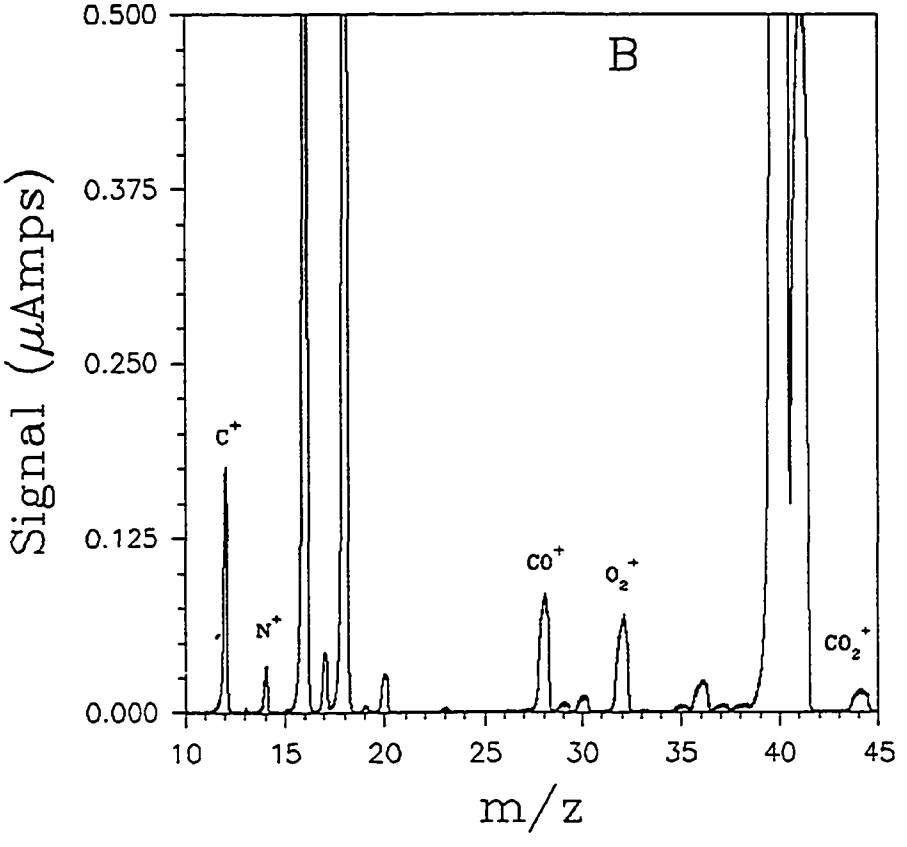

Fig. 2 (continued)

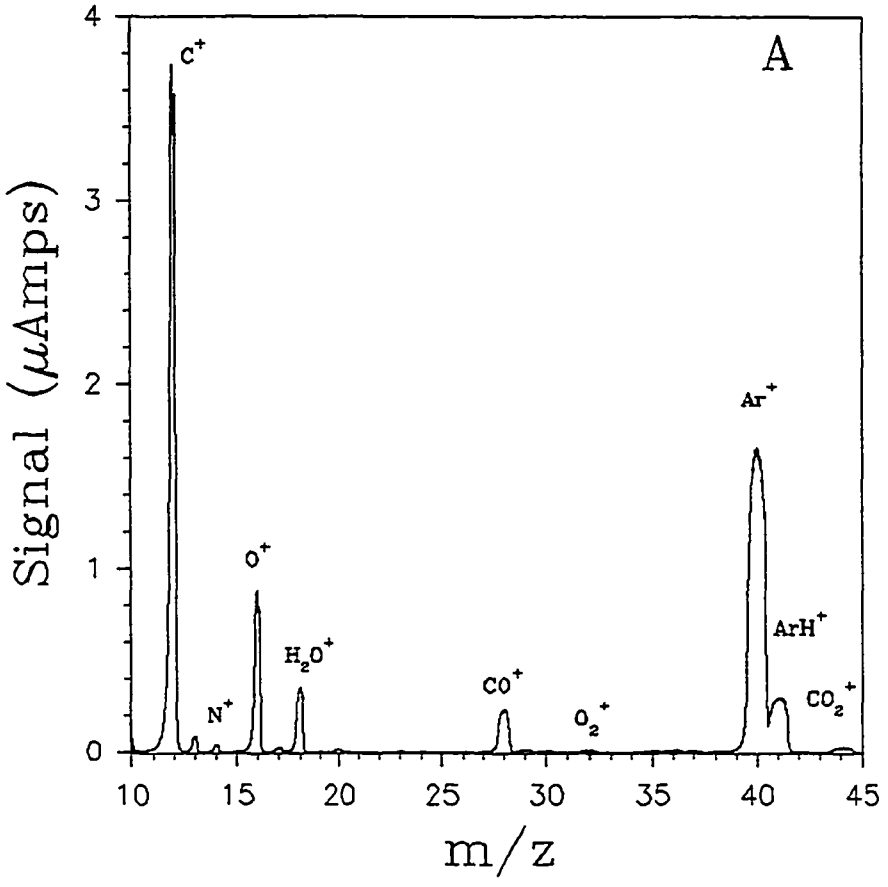

Figure 3. Background spectrum of deionized water while using a graphite injector made of spectroscopic graphite (SG).

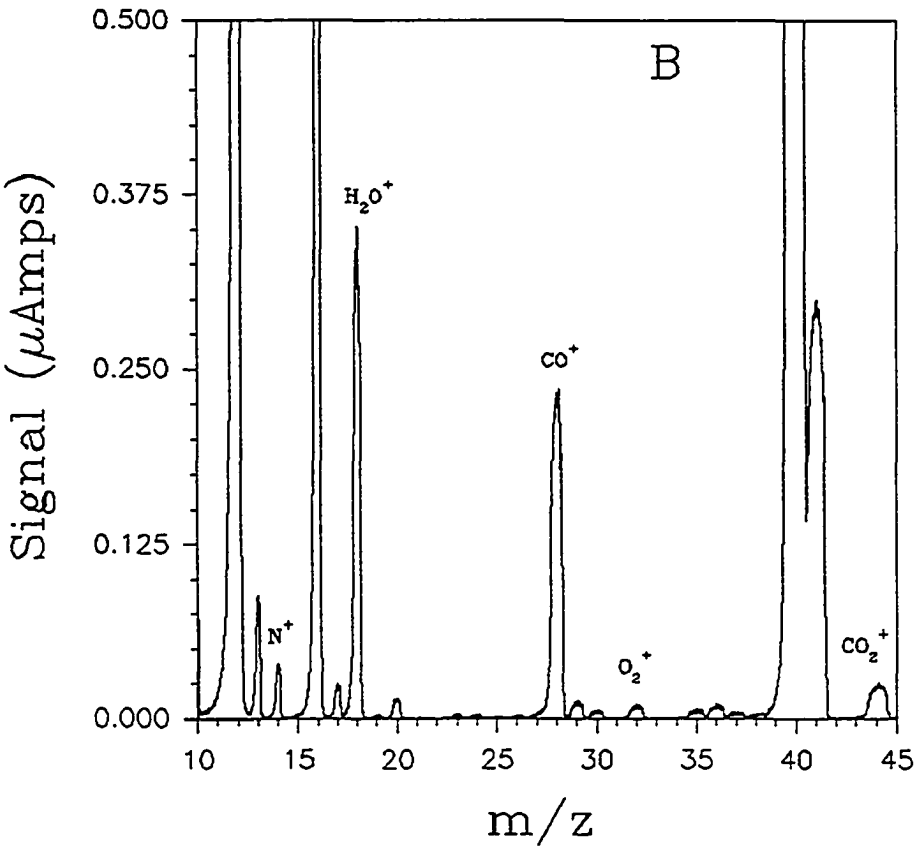

Fig. 3 (continued)

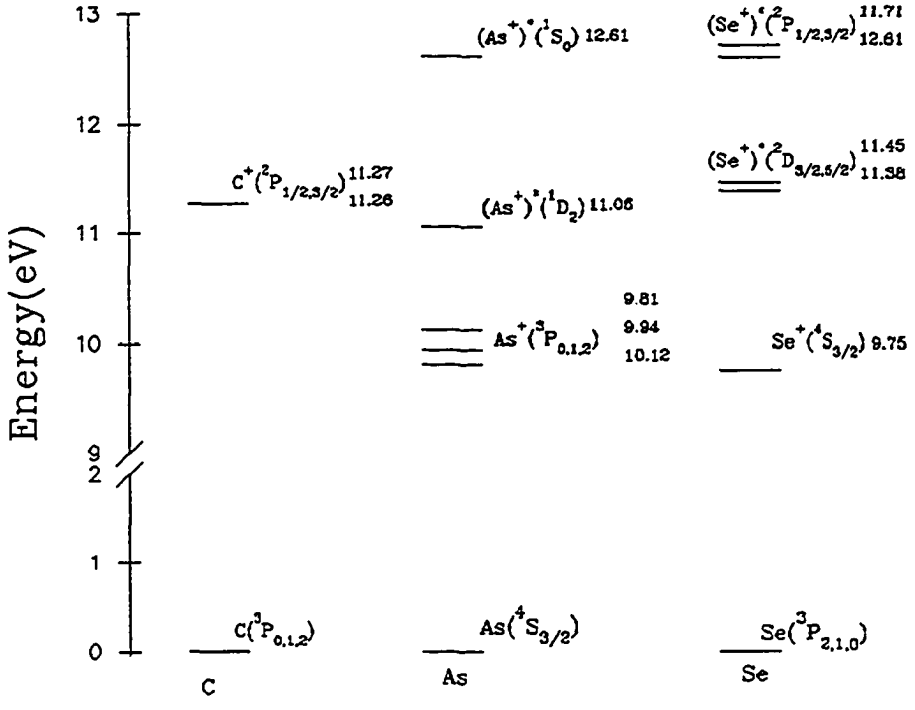

Figure 4. Partial energy diagram for C, As and Se. The energies of the first excited state of As^+ and Se^+ are close to the ground electronic state of C^+.

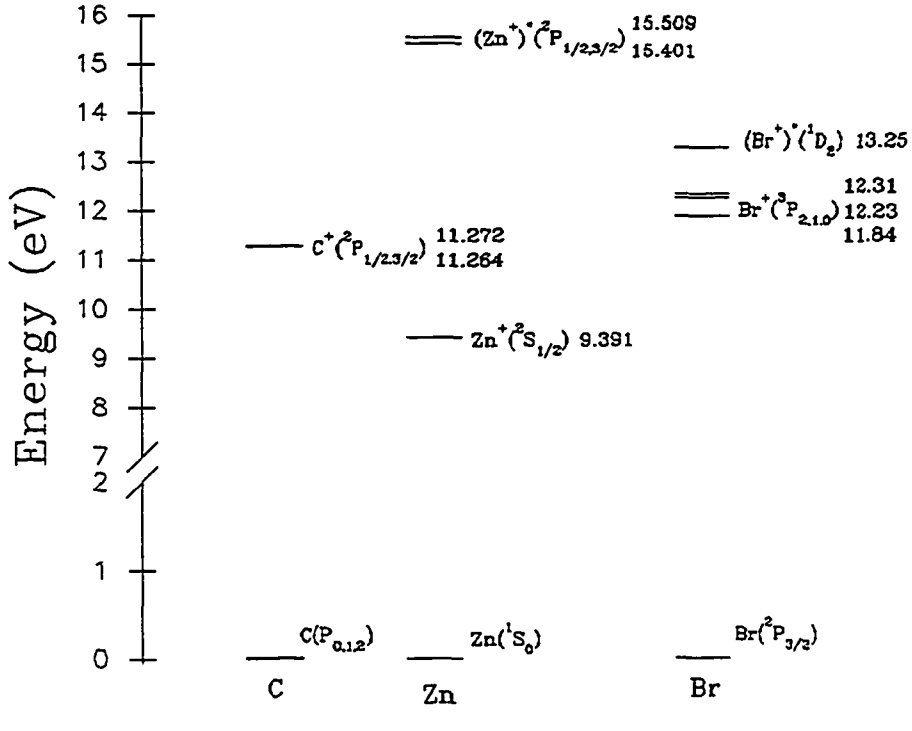

Figure 5. Partial energy diagram for C, Zn and Br. The energy defect between Zn^+ and C^+ is fairly large (1.87 eV). The lowest level of Br^+ is 0.58 eV above that of C^+

CHAPTER 5. GENERAL CONCLUSIONS

A new injector device for ICP-MS was introduced. This device consists of a support tube (stainless steel or alumina) with a graphite tube press fit into one end. The injector tube is supported by a tapered Teflon plug which fits into a demountable torch. This device is positioned such that the graphite tip protrudes into the axial channel of the plasma about 8 mm. A low MO^+ signal is achieved under operating conditions (aerosol gas flow rate, forward power and sampling position) that yield a maximum M^+ signal while using an ultrasonic nebulizer with desolvation. The MO^+/M^+ ratio is about 0.05% which is very similar to that obtained when using a normal quartz injector (QI) and cryogenic desolvation.[1] When cryogenic desolvation and the graphite torch injector (GI) are used together a MO^+/M^+ ratio of about 0.01% is obtained. Another advantage of this device is that sensitivity for atomic ions improves by a factor of 1.5 to 15, with the best improvements for elements like As and Zn that have high ionization energies. The graphite tube erodes and is useful for about 6 to 8 hours, or one day. Despite this degradation short and long term precision are not compromised. A rinse out curve shows that despite using a much lower aerosol gas flow rate (0.4-0.6 L min^{-1}) memory is not a serious problem.

This work also investigated the polyatomic ion background produced by this device. The low mass background spectrum shows C^+ is a dominant ion. In addition, CO^+ at m/z= 28 is quite prominent while the signal for O_2^+ is almost attenuated to near background levels. Background equivalent concentrations (BEC) are used to describe the mid-mass polyatomic ions. The BEC level for ClO^+ and $ArCl^+$ is about ten times lower with the GI compared to a QI. The BEC for $^{40}Ar^{12}C^+$ is about 10 times greater with the GI over the QI. This could be detrimental in determining $^{52}Cr^+$ but with the low BEC for ClO^+, $^{53}Cr^+$ becomes an available isotope. $^{40}Ar^{16}O^+$ does not behave like the metal oxides with a BEC level two times greater with a GI over a QI. Sample introduction methods that use a metal loop or cup produce background ions of the metal.[2] A stainless steel support tube produced background iron ions so it was replaced with an alumina tube. Absolute and relative levels of doubly charged ions are much higher for elements with low 2nd ionization energies when using a GI. Fortunately, the number of elements affected by interfering M^{+2} are few[3]. Matrix effects are similar to those reported previously with this instrument[4]. This problem can be eliminated by optimizing lens potentials for an analyte with the matrix element present. These results indicate a single internal standard can be used regardless of what matrix elements are present.

The last paper provides an explanation of how this device works. A correlation was made to the amount of carbon in the plasma and the level of MO^+ ions in the spectrum. The low relative metal oxide levels produced with this device are a result of two factors: (1) the narrow NAZ allows the sampling cone to collect ions further away from the oxide abundant IRZ; (2) the carbon of the graphite produces a reducing atmosphere much like that of a graphite furnace used in atomic absorption.[5]

This work did not investigate the location of the reaction involving carbon and metal oxides. There are two possibilities: (1) on the inside surface of the graphite tube; (2) by carbon condensation on the surface of vaporizing metal oxide particles. The first possibility is accepted as the mechanism that occurs with a graphite furnace. The second suggestion could be tested by observing the MO^+ signal produced from metal oxides of greatly different boiling points. A metal oxide with a high boiling point would not produce a cool neighborhood for carbon to condense on the oxide surface. The MO^+ signal should be higher than from a metal oxide with a lower boiling point. The increased analyte signals are partly attributed to more efficient collection of ions by the sampling cone due to the narrowing of the NAZ.

Some analyte signals (As and Se) are also enhanced by undergoing a charge transfer reaction with C^+. These elements

have ions with excited electronic states that are close (<0.5 eV) in energy to the ground state carbon ion. Their signals are related to the density of C^+ in the plasma. Elements (Zn and Br) that have ions with larger energy defects with C^+ show no signal dependence on C^+ density in the plasma.

This device is promising for determination of elements that are plagued by MO^+ interference. Future work should include a demonstration of this ability. A direct determination of high mass rare earth elements (HREE) in a matrix of low mass rare earth elements (LREE) would be a worthy experiment. Generally, this task requires mathematical corrections for removing the interfering MO^+ contribution to an analyte signal.[6] Future work should also include using the graphite injector with an axially viewed ICP-AES instrument. Matrix effects observed with an axially viewed plasma are partly caused by the emission resulting from the IRZ. As the matrix concentration increases the plasma is cooled due to the energy used for vaporization and atomization which results in more atom emission. The graphite injector produces a much smaller IRZ and could possibly mitigate matrix effects observed with this orientation.

References

1. Alves, L.C.; Wiederin, D.R.; Houk, R.S. *Anal. Chem.* 1992, 64, 1164.

2. Karanassios, V.; Horlick, G. *Spectrochim. Acta*, Part B, 1989, 44B, 1361.

3. Jarvis, K.E.; Gray, A.L; Houk, R.S *Handbook of ICP-MS*, Blackie, London 1992, Ch. 5.

4. Hu, K.; Houk, R.S. *J. Amer. Soc. Mass Spectrom.* 1993, 4, 28.

5. Chakrabarti, C.L; Chang, S.B; Roy, S.E. *Spectrochim. Acta*, PartB, 1983, 38B, 447.

6. Longerich, H.P.; Fryer, B.J.; Strong, D.F.; Kantipuly, C.J. *Spectrochim. Acta*, Part B, 1987, 42B, 75.

ACKNOWLEDGMENTS

I greatly acknowledge my major professor, Dr. R. S. Houk. When it appeared I was not capable of being successful in graduate school he gave me a chance. Through his support, tolerance and guidance this work became possible.

The machinists of the Ames Laboratory provided technical skill and relaxing conversation. I wish to express my appreciation to Jerry, Steve and all the members of the machine shop. Your help, kindness and assistance were quite valuable.

I would like to thank the members of the Houk group for their assistance and friendship: Dan Wiederin, Ke Hu, Fred Smith, Sam Shum and Rocky Warren. In addition, I would like to thank Shen Luan, Xiaoshan Chen, Lloyd Allen, Tonya Bricker and Ho-ming Pang for sharing their knowledge in the numerous conversations we had. I appreciate the kindness expressed by Steve Johnson for allowing me to stay with him during my last days in Ames and his comraderie on the softball field. We were once intramural champs, regardless of how it happened! Sam really showed his range at second base during that game.

To those who introduced me to what Iowa hunting and fishing have to offer, I thank you. I thank Ken Ewing for inviting me to hunt on his land. Furthermore, you proved that even a farm boy like me can be tested by the hot humid days of Iowa. The fruitful pheasant hunts with Lloyd Allen and Stan

Bajic provided a pleasant break, I hope I left a few for you. I wish to thank Darin St. Germain for taking me ice fishing in Minnesota. We didn't catch many but I'm glad you taught me the proper way to ice fish.

A special thanks goes to Amy and Dr. Brian Lamp and their families. Your friendship was key to helping Pam and I adapt to living far from our families, we can never thank you enough.

My friends and collegues at OSRAM Sylvania deserve acknowledgement for their support and patience. I apologize for not coming to you with the degree I had promised. Completion of this dissertation would not have been possible without your tolerance of my disposition.

This work was performed at the Ames Laboratory under contract no. W-7405-ENG-82 with the U. S. Department of Energy. I also wish to thank the Advanced Ceramics Corp. for donating the pyrolitic graphite used in this work.

I am very grateful to my parents, Thomas and Janet Clemons. My success is a testament to the love and support you have given to me through all my endeavors, regardless of merit. I am greatful to all my brothers and sisters, your successes and failures have helped guide me. I especially wish to thank Dr. Curtis Clemons for sharing helpful hints, and professional experience through my years in graduate school. I thank Gary and Wanda Schnell for their generosity

and kindness since I married their daughter.

Above all, I wish to acknowledge my wife, Pam. Five years of sacrifice, encouragement, patience and love have helped us achieve what seemed impossible. I thank my son Caleb for reminding me that an imagination is the heart of creativity and the best ideas begin with simple thoughts.